The authors thank the reviewer for their insightful comments and useful suggestions. We have provided a point-by-point response below.

Reviewer 1

This manuscript by Wong et al. investigates the evolution of water-soluble brown carbon (BrC) light absorption due to photolysis and OH oxidation for both laboratory generated BrC from the pyrolysis of cherry hardwood and ambient biomass-burning BrC collected in Crete. The results show interesting behavior starting with increase in absorption (photoenhancement) followed by decrease in absorption (photobleaching). The rates of these two stages were observed to depend on molecular weight, with larger molecules (> 400 Da) dominating the contribution to light absorption after several days of UV exposure. This is a well-written manuscript addressing a timely topic, and the findings constitute a step forward in the understanding of the evolution of atmospheric BrC. Therefore, I believe this manuscript is suitable for publication in ACP after the following comments are addressed:

1. It is not clear why both water and methanol extractions were performed for ambient samples and just water for laboratory samples. Please provide justification.

Response: We only focused on water extractions for laboratory sample since results from our previous work (Wong et al., 2017) indicated that the majority (77%) of the light absorption for laboratory generated BrC from wood smoke was contributed by the water-soluble fraction. This was stated in the original manuscript from lines 8-10. We also note that the trends in the evolution of light absorption for the methanol extraction for laboratory samples due to photochemical aging was also observed to be similar to the observations for water-soluble BrC fractions. We have modified section 2.1.1 (experimental section), as follows: "For these laboratory studies, we only focused on the aging of WS BrC, as results from our previous work indicated that the majority of the light absorption of laboratory generated BrC from wood smoke was contributed by the WS fraction (~ 77%) and that the trends in the evolution of light absorption of water-insoluble (i.e., methanol extracted) BrC due to photochemical aging are similar to that of the WS fraction (Wong et al., 2017)."

2. In section 2.1.1, it is stated that the BrC was produced by pyrolysis of cherry hardwood at 210 C and oxygen-free conditions. Is there a rationale behind choosing these conditions? It is known that the physicochemical properties and optical properties of BrC depend strongly on burn conditions (e.g. Chen and Bond (2010); Saleh et al. (2014); Pokhrel et al. (2016), etc.). While this is somehow acknowledged in the last sentence of the manuscript, the limitations of using one fuel and one burn condition should be featured early on when discussing the results (i.e. in section 3.1) as well as the abstract. This is not to take anything away from the interesting findings of this study.

Response: BrC was pyrolysed at 210°C under oxygen-free atmosphere to represent the smoldering conditions of wildfires, which we now have modified section 2.1.1 (experimental section) to mention this, as follows: "Wood smoke BrC was generated in the laboratory using the method described in Wong et al. (2017). Briefly, a small piece of dry cherry hardwood (5 - 10g), placed on the bottom of a cylindrical electronically-heated combustor, was pyrolyzed

under an oxygen-free atmosphere at 210°C, to representing BrC emitted from smoldering combustion (Andreae and Gelencsér, 2006; Chen and Bond, 2010)."

We have also added the following statements in the specified sections of the manuscript to emphasize the use of one fuel type and burn conditions for the laboratory generated BrC:

Abstract: "Here we report laboratory experiments that examined changes in the optical properties of the water-soluble BrC fraction of laboratory generated biomass burning particles from hardwood pyrolysis."

Section 3.2.1 (Results and discussion): "Firstly, the laboratory constrainted atmospheric lifetime represents BrC emitted from the combustion of one biomass fuel type under smoldering conditions, which may not represent ambient fire conditions, as the light absorption properties of BrC have been observed to be dependent on field and burn conditions (Chen and Bond, 2010)."

3. Section 3.1.1: Describe how MAC is calculated. The reference to Wong et al. (2017) is not enough, as this is a central piece of this paper and it will benefit the reader to have at least a brief explanation of how MAC is calculated.

Response: We have now described how the MAC values were calculated in section 2.1.4 (experimental section), as follows: "The measured light absorption for both bulk and molecular weight separated WS-BrC were normalized by the WSOC concentration of the BrC extract to represent the light absorption per water-soluble organic carbon, or mass absorption coefficient (MAC) of the WS-BrC."

We have also added the following to section 2.2.2 to describe the calculation of MAC for WS and MeOH BrC for the ambient filter samples: "The MAC of the WS and MeOH soluble BrC were determined through normalizing by the WSOC concentration (WS BrC/WSOC) or OC concentrations (MeOH BrC/OC), as determined using the TOC and OCEC analyzers, respectively."

4. Also, you need a short discussion of the meaning of MAC in this context. I assume this is a "bulk" MAC, which is related to but not the same as the MAC of suspended particles. See, for example, discussion in section 3.1.2 of Laskin et al. (2015).

Response: We have now added the following to section 3.1.1 to emphasize that the MAC represents the light absorption of the WS-BrC extract, "Note that these MAC values arise from light absorption measurements of water-extracted BrC and not of suspended BrC particles."

5. Finally, there is an inconsistency between the terminology in the text (MAC) and Figure 2 (AbsWSOC).

Response: We have now modified the Figure 2 such that Abs/WSOC is now referred to MAC.

6. While the molecular-weight separated results are interesting, I believe further discussion is required. First, it would be helpful to include a more detailed description of the SEC technique. In particular, the dependence of MW on elution volume (from Figure 3) seems to be very non-linear. Please elaborate more on this and how it affects the measurements.

Response: We agree that a discussion on the SEC technique would be helpful for readers, and have added a discussion of the SEC technique in section 2.1.4 (experimental section) as follows: "The molecular weight distributions of WS BrC were determined using size exclusion chromatography (SEC), which separates analyte molecules due to differences in the extent of permeation into the column packing material, where larger molecules elute earlier than smaller molecules due to weaker interactions (Strigel et al., 2009). The technique was operated using high-performance liquid chromatography (HPLC; GP40 Dionex), equipped with a SEC column (Polysep GFC P-3000, Phenomenex) that was operated in isocratic mode using a 90:10 *v/v* mixture of water and methanol with 25 mM ammonium acetate as the mobile phase, at 1mL min^{-1}."

We note that the elution time and molecular weight appears to be non-linear for Figure 3 because the relationship is linear for the logarithm of elution time to molecular weight. Since the elution of molecular weight separated BrC requires the use of a mobile phase, these dilution effects need to be account for in order to relate the absorbance of the molecular weight separated BrC to that of the bulk BrC sample. Since we have discussed these calculations in detail in our previous work (Wong et al., 2017), we have now added the following brief description in the section 2.1.4 (experimental section): "The absorbance of the different molecular weight fractions were determined by integrating the absorbance of a specific wavelength over the period of elution that corresponds to the molecular weight fraction ($P_{MW,\lambda}$). Since the coupling of the chromatographic technique to UV-VIS absorption measurements leads to the dilution of the BrC sample due to the use of the mobile phase, the absorbance of the molecular weight separated BrC is related to absorbance of the injected BrC by accounting for the mobile phase flow rate (*f*) and the volume of the injected BrC sample (V_{BrC}) using Eq. (1) :

$$A_{BrC,\lambda} = \frac{P_{MW,\lambda} \cdot f}{V_{BrC}} \qquad (1)"$$

New reference added: Strigel, Andre M., Yau, Wallace W., Kirkland, Joseph J. and Bly, Donald D.: Modern Size-Exclusion Liquid Chromatography, Second Edition., John Wiley & Sons, Inc., 2009.

7. Second, what is the rationale behind a) grouping into just low and high MW (why not low, medium, and high, for example?) and b) choosing 400 Da as the cutoff?

Response: The total light absorption was binned into two groups (high- and low-MW) instead of three because it is more reflective of the SEC separation process and better emphasize the uncertainties associated with the molecular weight information, as the accuracy of the SEC calibration approach, from which the MW information derives from, depends on whether the molecular densities of the calibration standards are representative of that of the BrC molecules. In other words, we feel the resolution of the SEC column combined with

uncertainties in calibration of the molecular weight separation does not warrant a more highly resolved classification then what we have used.

400 Da was designated as the cutoff for high- and low-MW BrC as it represents the penetration limit of the SEC column used.

8. Finally, Figure 3b shows that BrC absorption is mostly due to molecules larger than 10,000 Da. The observation of these large molecules, on its own, should be highlighted and discussed. Have such large molecules been observed in biomass burning BrC before?

Response: Ambient BrC molecules of molecular weights larger than ~10K Da have been previously observed in aged biomass burning aerosols collected at St. John's, Canada by De Lorenzo et al., 2017. We have highlighted this previous observation of high-MW BrC in the introduction and conclusion sections. We also note that given the large molecular weights and solubility in water, the high-MW BrC is likely to be of low-volatility, of which extremely low volatility organic compounds (ELVOCs) have been shown to dominate the light absorptivity of wood smoke BrC (Saleh et al., 2004). We have also added this point to the section 4 (conclusions and atmospheric implication).

References:

Chen Y, Bond TC (2010) Light absorption by organic carbon from wood combustion. Atmos Chem Phys 10(2001):1773–1787.

Saleh R, et al. (2014) Brownness of organics in aerosols from biomass burning linked to their black carbon content. Nat Geosci:DOI: 10.1038/NGEO2220.

Pokhrel RP, et al. (2016) Parameterization of single-scattering albedo (SSA) and absorption Ångström exponent (AAE) with EC/OC for aerosol emissions from biomass burning. Atmos Chem Phys 16(15):9549–9561.

Laskin A, Laskin J, Nizkorodov S a. (2015) Chemistry of Atmospheric Brown Carbon. Chem Rev:DOI: 10.1021/cr5006167.

The authors thank the reviewer for their insightful comments and useful suggestions. We have provided a point-by-point response below.

Reviewer 2

The authors present results from lab and field observations of absorption by brown carbon, generated from pyrolysis (lab) or from ambient fires (field). The lab experiments are well-done, although limited in scope given the focus on one source type (wood pyrolysis) that the authors have previously studied using similar methods (Wong et al., 2017, ES&T). Nonetheless, I believe the lab results are sufficiently novel and publishable after the authors address the reviewer comments. Regarding the field observations, I am much more skeptical of the results as they are currently presented and suggest they are removed unless further justification can be provided to provide a preponderance of evidence that they are correct for the reasons put forward.

In the intro (P2/L30 or so), the authors might consider also mentioning results from one of their earlier studies, Zhang et al. (2017, Nat. Geosci.).

Response: We have highlighted the results from our earlier work (Zhang et al., 2017) at the first paragraph of the introduction section in the original manuscript.

P3/L15: It is not clear to me that the Zhou study observed "negligible concentrations of levoglucosan" in aged BBOA. They saw a small f60 in their AMS mass spectrum for the BBOA-3 factor. F60 is not the same as levoglucosan. It is also not completely clear, to me at least, that the Zhou BBOA-3 factor doesn't include secondary formation, given the extremely large O:C. The same comment applies to the Bougiatioti et al. study. Their BBOA factor is transformed over time to an "OOA" factor, but it is also not clear whether this completely excludes the influence of secondary formation: factors cannot tell one directly about the processes that led to their occurrence. The use of f60 is problematic simply because it can vary as a result of dilution by secondary material in addition to heterogeneous oxidation.

Response: We agree with the reviewer that f60 is not the same as levoglucosan. We have now modified the sentence to clearly indicate that the studies of Zhou et al., and Bougiatioti et al., reported negligible mass spectrometric signatures of levoglucosan (i.e., f60), as follows: "Given that the average lifetime of atmospheric aerosols with respect to deposition is considerably longer, and that recent field observations have demonstrated aged BBOA had negligible concentrations of levoglucosan or of its mass spectrometric signatures (Bougiatioti et al., 2014; Zhou et al., 2017; Theodosi et al., 2018), these results suggest levoglucosan or mass spectral fragments cannot be used to estimate BrC levels in aged biomass burning emissions (> 1 day)."

In describing their "biomass burning" in the abstract and introduction (P3, L18) I suggest that the authors identify this as "biomass burning particles produced from pyrolysis." It is, in my view, critical that the source of the BB particles be clearly identified for lab studies so that the reader, in the abstract, can begin to think about how this study compares to others. This is also important because the authors produce their BB particles under oxygen free conditions. It is not clear to me the extent to which this leads to the production of particles that are broadly representative of

particles produced from open combustion, which includes oxygen. I suggest that the authors also comment on how representative they believe the particles produced from pyrolysis under oxygen free conditions to be.

Response: We agree that it should be highlighted in the abstract and introduction that the laboratory experiments were conducted on biomass burning particles emitted from biomass pyrolysis. The biomass burning particles, generated under oxygen-free condition, represents the smoldering phase of wildfires (Andreae and Gelencsér, 2006; Chen and Bond, 2010). We have now modified the manuscript to clarify these points (see response to Reviewer #1, question 2).

References:

Andreae, M. O. and Gelencsér, A.: Black carbon or brown carbon? The nature of light-absorbing carbonaceous aerosols, Atmos Chem Phys, 6(10), 3131–3148, doi:10.5194/acp-6-3131-2006, 2006.

Chen, Y. and Bond, T. C.: Light absorption by organic carbon from wood combustion, Atmos Chem Phys, 10(4), 1773–1787, doi:10.5194/acp-10-1773-2010, 2010.

P4/L10: The authors note that most absorption comes from WSOC (77%). However, given that they find differences in behavior between different WSOC fractions, the potential for the non-WSOC to behave differently than the WSOC seems large. Can the authors comment on this?

Response: In our previous work (Wong et al., 2017), we observed that the trends in the evolution of light absorption for the methanol extraction for laboratory samples due to photochemical aging by UVA aging was also observed to be similar to the observations for water-soluble BrC fractions. We have now added this point to the experimental section (please see response to Reviewer #1, question 1).

Figure S1: I think this would be better if the y-axis were a log scale, allowing the reader to compare at lower wavelengths better.

Response: Both UVA and UVB have similar photon fluxes at the smaller wavelengths and UVA lights have a much higher photon flux at longer wavelengths (as shown in Figure S1). As such, we believe that representing the axis for wavelength in a non-log scale is appropriate.

P8/L4: It would be helpful to the reader if the authors were to comment here on the extent of the losses. While some loss is evident, it is also clear that over the first 20 h period the extent of loss is quite small (5%?). Also, the vials used for the experiments were sealed with Teflon-lined caps. Given this, where do the authors suspect the losses occurred? Did highly volatile vapors leave escape through the caps?

Response: We have added and modified the discussion to mention the specific losses in WSOC that occur upon photochemical aging, as follows: "Upon illumination by UVB lights, losses in WSOC were observed for both direct UVB photolysis and UVB + H_2O_2 experiments (Figure 2a), with the majority of this loss occurring following 20 hours of illumination."

We can estimate the volume of the OC that partitioned into the gas-phase using the ideal-gas law: for a 30% loss of WSOC after 100 hours of illumination, with the WSOC concentration of the unreacted BrC solution (as mentioned in section 2.1.4 in the manuscript) at the room temperature and pressure, and assuming that the vapors have an average molecular weight of 200 g/mol, the vapors would have a volume (<0.1 uL), which is much less than the headspace of the glass vial. From this back-of-the-envelope calculation, the WSOC that was lost from the aqueous-phase (as highly volatile vapors) would have likely partitioned into the headspace of the 2mL sealed glass-vials (note that each vial originally contained 1 mL of the water extract of the laboratory generated biomass burning particles).

P8/L13: The authors state: "Given that a loss in WSOC was observed during this photoenhancement period, the increased MAC values may be driven by a loss in nonabsorbing WSOC and/or the formation of more absorbing WS BrC." I find this argument to be relatively weak because the extent of increase (factors of 2) is substantially larger than the loss in WSOC mass (_5%).

Response: This is a good point and should be highlighted in the discussion. We have now added the following discussion to section 3.1.1: "This initial increase in MAC values is likely driven by the formation of more absorbing WS BrC, as MAC values increased by a factor of ~ 2 while WSOC decreased only by factor of less than 1.1."

P8/L14: The authors indicate that the MAC increase with H2O2 was similar to that from UVB only. I agree that they are "similar" but it does seem that the changes in the H2O2 experiment was systematically larger. This is also connected with their observation of a steeper slope for H2O2 once things start to decline.

Response: We note that this part of the discussion pertains to the first 10 hours of the photochemical aging experiments. We have modified this sentence to clearly state that the changes in WSOC and MAC are similar for UVB and UVB + H_2O_2 experiments during this initial period of photochemical aging.

Abstract/L23: I suggest being more specific than "a few" hours. I would take this to mean around 3 h. Someone else might have a different number in mind. I suggest the authors just say over _10 h (or whatever the right values are to insert). A numerical scale is given for the decay, so should be given for the rise as well. Also, the "rapid photobleaching" of the low-MW stuff doesn't seem to really capture the overall behavior, which has multiple components, including a slower component. I suggest that this is revised to more fully capture the behavior shown in Fig. 4

Response: This is a good point. We agree that the timescale for the photoenhancement of high-MW BrC due to photochemical aging should be indicated. We have now modified the abstract to specify that the initial photoenhancement occurred up to ~ 15 hours. We have also specifically indicated that the majority of low-MW BrC undergo rapid photobleaching.

Data fitting: The authors extracted photoenhancement and photobleaching rate coefficients by fitting over different time periods. If the model proposed were robust, the authors should be able to describe the entire curve by fitting to both simultaneously. By fitting to separate regions, there

is a strong assumption that there is no overlap in terms of the processes. Yet, they must overlap to obtain the flat-top region. I suggest it would be better if the authors were to perform a comprehensive fit across the entire data set to extract their parameters, showing the results of the fitting on the associated graphs. This would help demonstrate the robustness of the model being used. Additionally, if the authors were to fit the observations using a more complete model they would not have to take a difference between the kUVB and kH2O2 to determine the OH-specific value. It would come naturally from fitting to the separate experiments. (Also, there appears to be a typo in Eqn. 2).

Response: Thank-you for pointing out the typo in Eqn. 2, which has been corrected. We also believe that the extracted rate constants from our current approach describes the *net* changes in light absorptivity due to photoenhancement and photobleaching processes, which can be directly compared to the field observations, which represent the net changes in light absorption due to either process. While we agree with that developing a more comprehensive kinetic model would extract more mechanistic information on the photoenhancement and photobleaching processes and should warrant further investigation. However, such a comprehensive kinetic model is not straight forward, two separate models will need to be develop, one for low-MW and one for high-MW BrC. Additionally, for the photoenhancement reaction, the relative light absorptivity between the original BrC reactant and the light absorbing product will need to be assumed – which is difficult given the fact that we do not know the concentration of the reactants vs. products (hence their molar-absorptivity). For these reasons, we decided not to use a more comprehensive model to estimate the photoenhancement and photobleaching rate constants.

P10/L5: Given the many commas in this sentence, I find it somewhat difficult to follow.

Response: We have now revised the sentence as follows: "For high-MW WS BrC, no differences in the evolution of their light absorption were observed between the two different photochemical aging experiments (Figure 4a). This suggests that their initial photoenhancement (up to 15 hours), and subsequent photobleaching, were only due to exposure to UVB radiation."

P10/L29: It is not clear how this indicates that changes occurred "only up to 500 nm". More convincing would be an actual plot of the MAC at 500 nm, showing that there is no photoenhancement. But the use of the AAE difference seems to me a more indirect way of getting at this when a direct method is available.

Response: We agree that differences in the changes in AAE values determined from different wavelength ranges can be used to assess spectral evolution of BrC due to aging, in addition to monitoring the evolution of MAC values at different wavelengths (approach that we demonstrated in Figure 2). We have now modified the statement to clearly indicate this, as follows: "Changes in the AAE values that were determined from different wavelength ranges can provide insight into the effects of photochemical aging on the light absorption spectral properties of BrC, in addition to monitoring the MAC values at different wavelengths."

Figures: On many, it would be helpful to the reader if tickmarks on the right sides were added.

Response: This is a great suggestion, we have now added tick marks to the right side of Figures 2, 4, 5, 6, and S6.

P10/L27: The "slight decrease" in the high-MW AAE is not abundantly clear to me, especially for the OH experiment. There's a quick drop but then an increase and at 10 h the AAE seems even higher than at the start. Also, are the error bars alluded to in the caption of Fig. 5 smaller than the data points? The somewhat random behavior of the low-MW data suggests that error bars are lacking.

Response: Thank-you for pointing this out. For Figure 5c, we have updated the scale for the y-axis such that the decrease in $AAE_{320\text{-}420nm}$ for high-MW WS BrC is clear. In addition, we now use shaded areas to present the experimental variability for Figure 5.

P11/L8: it is not clear to me how the authors are concluding that OH is the dominant loss mechanism. Fig. 4 shows that the low-MW stuff decays both from the UVB experiment and the OH experiment to similar extents.

Response: Aqueous OH oxidation was determined to be the dominant loss mechanism for the less reactive fraction of low-MW WS BrC as it resulted in the shortest estimated atmospheric lifetime compared to the other aging mechanisms studied in the laboratory (listed in Table S1).

Field observations: I do not find the results presented especially compelling. There are two individual points for the WSOC MAC showing the increase. The data points around these two do not show evidence of any continuous evolution over time. Instead, there is a step function.

Response: We agree that the evolution of WS BrC MAC appears to be a step function – a initial increase from 0 to 8 hours of atmospheric transport, followed by a decrease in MAC for WS BrC with atmospheric transport times of about 15 hours. We have discussed this trend in the original manuscript.

And this step function is not seen with the MeOH MAC values. (Also, the increase in the MeOH absorption the authors mention at 10 h is not apparent to me. It seems to be flat within the data variability.)

Response: We agree that the increase in MeOH BrC MAC values from 1 to 8 hours of atmospheric transport times is cannot be discern given the variability of the whole dataset. We have now explicitly stated this in section 3.2.1.

What can I take the uncertainty as on these measurements?

Response: The error bars for the filled points presents the interquartile range of the data points within a specific bin of atmospheric transport times.

What should I make of the WSOC being substantially higher than the OC at the 33 h point in terms of uncertainty? What steps have the authors taken to convince themselves that this is not some artifact?

Response: Thank-you for pointing this out. We have taken the following quality assurance and quality control measures for field samples:

1) **multiple blanks were collected throughout the campaign to identify potential sampling contamination and limits of detection (LOD). The LODs (3 times the standard deviation of field blanks) were determined to be 0.30 µgC m^{-3} for WSOC and 0.88 µgC m^{-3} for OC, 1.7 x 10^{-7} m^{-1} for WS BrC light absorption, and 3.8 x 10^{-7} m^{-1} for MeOH light absorption. Only samples above LOD were used for further analysis.**
2) **more than half of the samples were analyzed in duplicates to assess reproducibility. Several filters samples from each fire season were also analyzed in triplet to quantify measurement variability. The measurement uncertainties were estimated to be 18% for WSOC/OC measurements, and 20% for the light absorption measurements (based on blanks, standards, and field samples duplicates).**

Unfortunately, the WSOC measurement for the filter sample of atmospheric transport time of 33 hours was only conducted once and as pointed out, we should have noted that this sample had WSOC > OC. We have reanalyzed the filter in question in triplet and have clearly identified that the previous observation was an outlier, and that from this reanalysis work, OC > WSOC for this sample. We have also repeated this process for all samples were that previously only analyzed once (ten in total). We note that with the exception for the filter sample of atmospheric transport times of 33 hours, all the other repeated measurements were within the reported variability (~ 20%). We have now updated all the corresponding data and figures. In addition, we now mention the LOD and uncertainties of our measurements in the experimental section of the revised manuscript.

Also, samples were collected for 22-24 h. Given this, what does it even mean to have an aging time of only 5 or 10 h? And were these daytime hours, given that there was sampling during day and night? If half the transport occurred at night, should the aging times be divided in two?

Response: The denoted atmospheric transport time for each filter sample is the average atmospheric transport time as determined from each hourly trajectory that was computed during each filter sampling interval (i.e., the average time for the airmass to be transported from the biomass burning site to the sampling site). Given that the samples were collected for a period of 22 – 24 hours, the atmospheric transport time can include both day and nighttime hours. We note there are nighttime aging processes that can transform the light absorptivity of BrC, such as dilution (McMeeking et al., 2014; Saleh et al., 2014).

References:

McMeeking, G. R., Fortner, E., Onasch, T. B., Taylor, J. W., Flynn, M., Coe, H. and Kreidenweis, S. M.: Impacts of nonrefractory material on light absorption by aerosols

emitted from biomass burning, J. Geophys. Res. Atmospheres, 119(21), 12,272-12,286, doi:10.1002/2014JD021750, 2014.

Saleh, R., Robinson, E. S., Tkacik, D. S., Ahern, A. T., Liu, S., Aiken, A. C., Sullivan, R. C., Presto, A. A., Dubey, M. K., Yokelson, R. J., Donahue, N. M. and Robinson, A. L.: Brownness of organics in aerosols from biomass burning linked to their black carbon content, Nat. Geosci., 7(9), 647–650, doi:10.1038/ngeo2220, 2014.

Did the backtrajectories indicate that the air reaching the sampling site had been at the surface where the fire was in all cases? HYSPLIT gives altitude as well as location.

Response: For filter samples that were influenced by biomass burning, all the corresponding back trajectories indicated that the airmasses were within 1000 m above ground level when they were at the biomass burning site. We note that the biomass burning plumes in Eastern Europe have been previously observed to have average injection heights of 3077 ± 951 m (Amiridis et al., 2010), so it is not necessarily the case that the airmass has to be at the surface to be influenced by the biomass burning emissions.

References:

Amiridis, V., Giannakaki, E., Balis, D. S., Gerasopoulos, E., Pytharoulis, I., Zanis, P., Kazadzis, S., Melas, D. and Zerefos, C.: Smoke injection heights from agricultural burning in Eastern Europe as seen by CALIPSO, Atmospheric Chem. Phys., 10(23), 11567–11576, doi:https://doi.org/10.5194/acp-10-11567-2010, 2010.

Also, were these two samples for the same fires as at shorter or longer times? What if the nature of the fire and combustion conditions differed? Saleh et al. (2014, Nat. Geosci.) showed that the MAC (or the equivalent imaginary component) for the BrC varies with the combustion conditions. How can the authors rule out changes in conditions? I need to be further convinced about this analysis overall. Currently, I do not think it is sufficiently supported to be included in the manuscript.

Response: For the samples that were included in the two MAC median values, they were all of different fires. We agree that the approach to identify biomass burning influence does not account for variability in BrC emissions from various fires, including duration, fire intensity, etc. We have stated these limitations in section 2.2.1 (experimental), as well as in section 3.2.1 (results and discussion). We also note that given the strong oxidizing environment of the Eastern Mediterranean, the field observations and their comparison to controlled laboratory photochemical experiments are valuable in evaluating the current understanding of the atmospheric evolution of BrC.

P12/L18: I have a hard time believing that the AAE values are inversely proportional to the BC-to-OA based on the data presented. In my view, the observations show zero relationship, and the range of BC/OA is too small to show a relationship anyway. And, the authors are not accounting for the potential for secondary formation in the atmosphere, which would skew the relationship. I think this discussion should be struck as Fig. S7 does not show what the authors purport. I would need to be convinced with an R^2 at minimum.

Response: It is a good point that from the current dataset, the relationship of AAE and BC-to-OA is difficult to discern, given the limited range of BC-to-OA ratios observed. We have removed Figure S7 and the associated discussion in the manuscript.

The authors might consider commenting on the typical amount of time that BrC spends in a cloud droplet, since their results are most relevant to material in cloud droplets.

Response: It is true that the BrC concentrations used in the laboratory experiment best represent those in cloud droplets. However, the aqueous aging chemistry investigated in this study can also occur in aqueous particles. We have noted in the original manuscript (section 3.2.1) that the laboratory work did not consider parameters that may affect the reactivity of ambient BrC in aqueous particles, such as viscosity, aerosol phase state, and solute concentrations.

Levoglucosan: To what extent is it known whether the amount of levoglucosan produced relative to all other OA (or to BrC specifically) is a constant across varying burn conditions? This seems important to me to consider to understand the different relationships. The "total" hydrous sugars, I would speculate, is more likely to be consistent between burns than is a single sugar. As is something like K+, which would be relatively independent of burn conditions (although would be fuel dependent). Nonetheless, the authors do convincingly show that the total sugars is more robust than levoglucosan alone.

Response: It is true that the emission of levoglucosan relative to OA and the relative emission of BrC to OA are not constant across varying burn conditions (Mazzoleni et al., 2007; Kalogridis et al., 2018) and could have led to the lack of correlation observed for BrC and levoglucosan. We have modified this section to include this point.

Added References:

Mazzoleni, L. R., Zielinska, B. and Moosmüller, H.: Emissions of Levoglucosan, Methoxy Phenols, and Organic Acids from Prescribed Burns, Laboratory Combustion of Wildland Fuels, and Residential Wood Combustion, Environ. Sci. Technol., 41(7), 2115–2122, doi:10.1021/es061702c, 2007.

Kalogridis, A.-C., Popovicheva, O. B., Engling, G., Diapouli, E., Kawamura, K., Tachibana, E., Ono, K., Kozlov, V. S. and Eleftheriadis, K.: Smoke aerosol chemistry and aging of Siberian biomass burning emissions in a large aerosol chamber, Atmos. Environ., 185, 15–28, doi:10.1016/j.atmosenv.2018.04.033, 2018.

It might be useful to know which two data points in Fig. 7 correspond to the two elevated MAC points in Fig. 6. It is not apparent than both of the elevated points are included in Fig. 7, because there should be two points with absorption > 2e-6 (from Fig. 6) but there is only one. The point that must be one of these is clearly one for which the relationship with levoglucosan is completely different than for any other points. Also for K+. This could indicate that the combustion conditions were, indeed, different for these high MAC points and thus that the elevated MAC was driven by differences in burn conditions and not aging.

Response: We note that only filter samples of atmospheric ages > 10 hrs (i.e., aged biomass burning emissions) were included in the analysis shown in Figure 7, as such, one of the filter samples with Abs_{365} > 2 e-6 m-1 were not included in Figure 7. It is true that the filter sample of high absorption corresponds to one of the elevate MAC values shown in Figure 6. It is a very good point that the relationship of Abs_{365} to levoglucosan and potassium is clearly different for this high Abs_{365} point compared to the rest of the data, which may suggest that the burning conditions for this filter sample is different.

There is no indication of where the data are archived, which I believe is now required by ACP.

Response: Thank-you for pointing this out. We have now provided all the data in a data repository. We have noted this in the section "Data Availability" at the end of the revised manuscript, before the acknowledge section.

Atmospheric Evolution of Molecular Weight Separated Brown Carbon from Biomass Burning

Jenny P.S. Wong[1], Maria Tsagkaraki[2], Irini Tsiodra[2,3], Nikolaos Mihalopoulos[2,4], Kalliopi Violaki[5], Maria Kanakidou[2], Jean Sciare,[6] Athanasios Nenes[1,3,4,7], and Rodney J. Weber[1]

[1]Earth and Atmospheric Sciences, Georgia Institute of Technology, Atlanta, 30331, USA
[2]Environmental Chemical Processes Laboratory, Department of Chemistry, University of Crete, 71003 Heraklion, Greece
[3]ICE-HT, Foundation for Research and Technology Hellas, Patras, 26504, Greece
[4]IERSD, National Observatory of Athens, Palea Penteli, 15236, Greece
[5]Aix-Marseille University, Mediterranean Institute of Oceanography (MIO) UMR 7294, University de Toulon, CNRS, IRD, France
[6]Energy Environment and Water Research Center, The Cyprus Institute, Nicosia 1645, Cyprus
[7]Laboratory of Atmospheric Processes and their Impacts, School of Architecture, Civil & Environmental Engineering, École Polytechnique Fédérale de Lausanne, Lausanne, 1015, Switzerland

Deleted: Tsagaraki[2]

Deleted: [7]School

Abstract

Biomass burning is a major source of atmospheric brown carbon (BrC) and through its absorption of UV/VIS radiation, it can play an important role on the planetary radiative balance and atmospheric photochemistry. The considerable uncertainty of BrC impacts is associated with its poorly constrained sources, transformations and atmospheric lifetime. Here we report laboratory experiments that examined changes in the optical properties of the water-soluble BrC fraction of laboratory generated biomass burning particles from hardwood pyrolysis. Effects of direct UVB photolysis and OH oxidation in the aqueous phase on molecular weight-separated BrC were studied. Results indicated that the majority of low molecular weight (MW) BrC (< 400 Da) was rapidly photobleached by both direct photolysis and OH oxidation on an atmospheric timescale of approximately 1 hour. High MW BrC (≥ 400 Da) underwent initial photoenhancement up to ~ 15 hours, followed by slow photobleaching over ~ 10 hours. The laboratory experiments were supported by observations from ambient BrC samples that were collected during the fire seasons in Greece. These samples, containing freshly emitted to aged biomass burning aerosol, were analyzed for both water and methanol soluble BrC. Consistent with the laboratory experiments, high MW BrC dominated the total light absorption at 365 nm for both methanol and water-soluble fractions of ambient samples with atmospheric transport times of 1 to 68 hours. These ambient observations indicate that overall, biomass burning BrC across all molecular weights has an atmospheric lifetime of 15 to 28 hours, consistent with estimates from previous field studies - although the BrC associated with the high MW fraction remains relatively stable and is responsible for light absorption properties of BrC throughout most of its atmospheric lifetime. For ambient samples of aged (> 10 hours) biomass burning emissions, poor linear correlations were found between light absorptivity and levoglucosan, consistent with other studies suggesting a short atmospheric lifetime for levoglucosan. However, a much stronger correlation between light absorptivity and total hydrous sugars was observed, suggesting that they may serve as more robust tracers for aged biomass burning emissions.

Deleted: over a few

Deleted: ten

Deleted: have

Deleted: 20

Overall, the results from this study suggest that robust model estimates of BrC radiative impacts require consideration of the atmospheric aging of BrC and the stability of high-MW BrC.

1 Introduction

Brown Carbon (BrC), the fraction of organic aerosol that absorbs solar radiation in the UV and near-visible wavelengths, may potentially be an important climate warmer with estimated direct radiative forcing that varies from +0.03 to +0.60 W m^{-2} (e.g., Park et al., 2010; Feng et al., 2013; Lin et al., 2014; Wang et al., 2014; Saleh et al., 2015; Jo et al., 2016), and a vertical distribution that can be distinctly different from black carbon and other climate warmers (Zhang et al., 2017). In addition to climate impacts, the importance of UV solar radiation for photochemistry also implies that BrC may affect atmospheric chemistry (He and Carmichael, 1999; Mok et al., 2016).

Current knowledge on the sources, sinks, optical properties and atmospheric lifetime of BrC is limited. Among the sources of BrC, combustion of biomass (Andreae and Gelencsér, 2006; Alexander et al., 2008; Hecobian et al., 2010; Kirchstetter and Thatcher, 2012; Saleh et al., 2014; Lack et al., 2012) and fossil fuels (Bond, 2001; Zhang et al., 2011) are thought to dominate; for example, over one year in SE USA, 50% of BrC was attributed to biomass burning (Hecobian et al., 2010). Secondary processes that often involve carbonyls and nitrogen-containing compounds can also generate BrC in the atmosphere (Laskin et al., 2015). Molecular identification of the chromophores is a challenging task, as there may be a multitude of light absorbing compounds. It remains unclear whether BrC is comprised of low concentrations of strongly absorbing chromophores, or a large number of weakly-absorbing chromophores in a complex organic matrix. To date, several classes of compounds have been identified as BrC in biomass burning organic aerosols (BBOA), such as nitroaromatic compounds (Desyaterik et al., 2013; Zhang et al., 2013; Mohr et al., 2013; Lin et al., 2016), humic-like substances (HULIS; Dinar et al., 2008; Hoffer et al., 2006; Fan et al., 2016; Wang et al., 2017), and other high molecular weight substances (i.e., compounds > 400 Da) (Di Lorenzo and Young, 2016; Di Lorenzo et al., 2017; Wong et al., 2017).

Studies have suggested that following the emission or formation of biomass burning BrC, their optical properties can be transformed by atmospheric aging processes. Laboratory studies, for both model compounds and complex mixtures of biomass burning BrC, suggested that initial stages of photochemical aging can increase light absorption ("photoenhancement"), followed by a subsequent decrease ("photobleaching") (Saleh et al., 2013; Zhong and Jang, 2014; Zhao et al., 2015; Sumlin et al., 2017; Hems and Abbatt, 2018). The atmospheric lifetime was constrained only for biomass burning BrC from nitrophenols, where photobleaching by aqueous OH oxidation in fog or cloud droplets was found to be their dominant atmospheric loss mechanism, with an estimated atmospheric lifetime of a few hours (Zhao et al., 2015; Hems and Abbatt, 2018). Field observations from wildfire emissions in the Northwestern USA and Amazon have suggested that most biomass burning BrC chromophores have an atmospheric lifetime in the range of 13 to 30 hours (Forrister et al., 2015; Wang et al., 2016). It was observed, however, that the majority of light absorption in aged biomass burning BrC (approximately 2 days of atmospheric transport) from wildfire emissions in Northeastern Canada, was associated with compounds of 500 Da and larger (Di Lorenzo

and Young, 2016; Di Lorenzo et al., 2017). Altogether, this indicated that a fraction of high molecular weight BrC is recalcitrant to atmospheric aging processes. While there is field evidence that aqueous-phase chemistry can transform the optical properties of BrC emitted from biomass burning (Gilardoni et al., 2016; Zhang et al., 2017), the specific aging processes leading to these field observations remain unknown. In addition, these contrasting laboratory and field observational constraints on the atmospheric lifetime of BrC are much shorter than the assumed atmospheric lifetime of BrC (approximately 4 days) utilized in models to estimate its impacts on aerosol direct radiative forcing (Jo et al., 2016).

Along with constraining the atmospheric lifetime of biomass burning BrC, accurate estimates of the contribution of biomass burning to global BrC are also critical for robust assessments of its climatic impacts. Levoglucosan, an anhydrous sugar emitted during biomass pyrolysis, is a molecular tracer widely used to estimate the contribution of biomass burning to ambient organic aerosol concentrations, as it was historically thought to be chemically inert (Simoneit et al., 1999). Yet, a growing number of studies have demonstrated that levoglucosan is subject to significant atmospheric loss, with an estimated atmospheric lifetime of 0.7 to 2.2 days (Hennigan et al., 2010; Hoffmann et al., 2010; Kessler et al., 2010; May et al., 2012; Slade and Knopf, 2014; Zhao et al., 2014; Sang et al., 2016). Given that the average lifetime of atmospheric aerosols with respect to deposition is considerably longer, and that recent field observations have demonstrated aged BBOA had negligible concentrations of levoglucosan or of its aerosol mass spectrometric signatures (Bougiatioti et al., 2014; Zhou et al., 2017; Theodosi et al., 2018), these results suggest levoglucosan or its mass spectral fragments cannot be used to estimate BrC levels in aged biomass burning emissions (> 1 day).

In this study, we systematically investigated the photochemical aging of molecular weight-separated water-soluble (WS) BrC fraction of biomass burning particles produced by wood pyrolysis, by both aqueous OH oxidation and photolysis by UVB radiation. We build upon earlier laboratory experiments that examined the aging effects of photolysis by UVA radiation (Wong et al., 2017) to establish a more complete understanding of the effects of different photochemical aging processes. Based on the photobleaching rates determined from these laboratory experiments, we estimated the dominant photochemical pathway leading to the loss of biomass burning BrC in the atmosphere. To provide additional field evidence of the impacts of atmospheric aging on biomass burning BrC, and to further assess the atmospheric stability of high molecular weight BrC, the light absorptivity of molecular weight-separated water and methanol (MeOH) soluble BrC fraction from ambient samples of different atmospheric ages was determined. Finally, from these ambient samples, we assessed the use of levoglucosan and other proposed biomass burning species as robust tracers for aged biomass burning aerosol and BrC.

Deleted: from

2 Experimental

2.1 Laboratory Experiments

2.1.1 Preparation of WS BrC

Wood smoke BrC was generated in the laboratory using the method described in Wong et al. (2017). Briefly, a small piece of dry cherry hardwood (5 - 10g), placed on the bottom of a cylindrical electronically-heated combustor, was pyrolyzed under an oxygen-free atmosphere at 210°C, to represent BrC emitted from smoldering combustion (Andreae and Gelencsér, 2006; Chen and Bond, 2010). The resulting smoke stream was subsequently diluted with filtered air by a factor of ~30 and the BBOA was collected on polytetrafluoroethylene filters (47 mm, 2µm pore size, Pall Corporation) at 6 lpm for 100 min and stored at -10°C. Prior to each laboratory experiment, water-soluble (WS) BrC was extracted from the filter by adding 15 mL of purified water (18.2 mΩ) in a sealed glass vial and sonicated for 60 min. The extract was filtered using a 0.2 µm PTFE syringe filter (Fisher) to remove any insoluble materials that may damage the chromatography column or plug the waveguide used to characterize BrC properties (Section 2.1.4). Given that the WS BrC is dissolved in bulk aqueous solutions, the experimental conditions for the photochemical aging experiments, such as BrC concentrations and viscosity, most likely represent the aging of WS wood smoke BrC in fog and/or cloud droplets. For these laboratory studies, we only focused on the aging of WS BrC, as results from our previous work indicated that the majority of the light absorption of laboratory generated BrC from wood smoke was contributed by the WS fraction (~ 77%) and that the trends in the evolution of light absorption of water-insoluble (i.e., methanol extracted) BrC due to photochemical aging are similar to that of the WS fraction (Wong et al., 2017).

Deleted: ..

Deleted:

Deleted: ..

2.1.2 Photolysis of WS BrC by UVB lights

Experiments examining the photolytic aging of WS BrC by UVB lights follow the same experimental procedure for UVA photolysis as described in Wong et al. (2017). All photochemical aging experiments were conducted in a photoreactor, with a slowly rotating vial rack (40 rpm) placed in the center and surrounded by 16 UVB lamps (Desert Series 50 T8, Zilla). With all UV lamps on, continuous ventilation by two fans maintained the temperature inside the photoreactor to 30 ± 1°C. The photon fluxes inside the photoreactor from UVB lamps were determined by chemical actinometry using 2-nitrobenzaldehyde (see Wong et al., 2017 for experimental details). The wavelength dependent photon fluxes from both UVA and UVB lamps are shown in Figure S1, where the actinic flux at solar noon is provided for comparison. Most of the radiation fell in the range of 300 – 400 nm, with a maximum at 355 nm and 310 nm for UVA and UVB lamps, respectively. Note that while both UVB and UVA lamps have comparably similar photon fluxes for wavelengths lower than 320nm, the UVA lamps have correspondingly much higher photon flux at higher wavelengths. These spectral differences allowed for investigating the wavelength dependence of BrC aging by photolysis.

For each photolysis experiment, multiple, pre-cleaned 2 mL borosilicate glass vials (sealed with Teflon-lined caps), each containing 1mL of the WS BrC extract solution, were placed on the rotating vial rack inside the photoreactor. Each extract

solution was diluted by 5% (with purified water) such that the final concentration of WS BrC used in the photolysis experiments are identical to those used in the aqueous OH oxidation experiments, where the WS BrC concentration was diluted by 5% from the addition of H_2O_2 (Section 2.1.3). The vials were illuminated by UVB lights for up to approximately 100 hours, where at different illumination times, one vial was removed for offline analysis (described in Sec. 2.1.4). Control experiments were conducted; no changes in WS BrC properties were observed when the vials containing the extract were completely covered by aluminium foil, where they were only exposed to the elevated temperatures inside the photoreactor, and not UVB radiation. Photolysis experiments were repeated at least 3 times to ensure reproducibility.

2.1.3 Aqueous OH Oxidation of WS BrC

Experiments for aqueous OH oxidation were conducted in the same experimental setup used in the photolysis experiments. H_2O_2 (30%, Sigma Aldrich) was added to the WS BrC extract solution (final concentration of 1.5 mM) as a photolytic source of OH radical upon irradiation with UVB lights (up to 18 hours). Dark control experiments were conducted to confirm that the dark reaction of H_2O_2 with WS BrC did not change its optical or molecular weight properties. Similar to photolysis experiments, at different illumination times, one vial was removed for offline analysis. The OH oxidation experiments were repeated 3 times to ensure reproducibility.

The steady-state OH concentration ($[OH]_{ss}$) in these photochemical oxidation experiments was determined in order to estimate the atmospheric lifetime of WS BrC with respect to aqueous OH oxidation. This was performed by monitoring the formation of para-hydroxybenzoic acid (*p*-HBA) from the reaction of OH with benzoate, a commonly employed OH scanvenger (Zhou and Mopper, 1990; Anastasio and McGregor, 2001; Badali et al., 2015). The OH quantification experiments are described in detail in Section S1. Briefly, sodium benzoate (0.1 – 1.0 µM) was added to WS wood smoke BrC extract solution with and without 1.5mM H_2O_2. The resulting solutions were illuminated for up to 18 hours, where at different times, a sample vial was removed to determine the concentration of *p*-HBA, using HPLC-UV/VIS absorption. The yield of *p*-HBA from the reaction of OH with benzoate (0.17) was used to convert the formation rate of *p*-HBA to an OH production rate, from which the $[OH]_{ss}$ was estimated. *p*-HBA does not absorb radiation in the same wavelength regions as BrC, but given that other products formed from the reaction of OH + benzoate do, in order to avoid measurement interference from these products, the OH quantification experiments were conducted separately from the experiments where the effects of OH oxidation on BrC properties were examined. In these experiements, the relationship between OH photo-production and benzoate concentration was determined in order to quantify $[OH]_{ss}$ in the aqueous OH oxidation experiments where the BrC properties were monitored (i.e., no benzoate as an added OH scavenger). Figure S2 shows the relationship between the *p*-HBA formation rate and concentration of added benzoate was used to estimate the $[OH]_{ss}$ when [benzoate] = 0 (i.e., experiments where light absorptivity of BrC was monitored).

2.1.4 Offline WS BrC Measurements

Following the removal of each sample vial from the photoreactor, the BrC solutions were divided to determine various BrC chemical and optical properties, using the same procedures outlined in Wong et al. (2017). Briefly, changes in the water-soluble organic carbon (WSOC) concentration due to photochemical aging were monitored using a Sievers Total Organic Carbon (TOC) Analyzer (Model 900, GE Analytical Instruments). For these measurements, the WS BrC samples were diluted by a factor of 250 to ensure the WSOC concentrations were in the linear range of the instrument, which was routinely calibrated using solutions of dissolved sucrose of known concentrations. Prior to photochemical aging, each sample vial contained 1400 ± 178 ppb of WSOC. The light absorptivity of WS BrC of all molecular weights (i.e., bulk WS BrC) was monitored using the 250x diluted WS BrC solutions and an absorption spectrometer consisting of a liquid waveguide capillary (2.5 m optical path-length, World Precision), a deuterium tungsten halogen light source (DT-Mini, Ocean Optics), and a light detector (USB4000, Ocean Optics) that can continuously monitor all wavelengths between 230 and 800 nm. The molecular weight distributions of WS BrC were determined using size exclusion chromatography (SEC), which separates analyte molecules due to differences in the extent of permeation into the column packing material, where larger molecules elute earlier than smaller molecules due to weaker interactions (Strigel et al., 2009). The technique was operated using high-performance liquid chromatography (HPLC; GP40 Dionex), equipped with a SEC column (Polysep GFC P-3000, Phenomenex) that was operated in isocratic mode using a 90:10 *v/v* mixture of water and methanol with 25 mM ammonium acetate as the mobile phase, at 1mL min^{-1}. The near-UV/VIS absorbance of the molecular-weight separated BrC compounds were monitored using an absorbance spectrometer that was coupled in-line with the SEC system. The spectrometer consisted of the same components as the one used for bulk WS BrC measurements, except a liquid waveguide capillary with a 1 m optical path-length (World Precision) and a different model of the deuterium tungsten halogen light source (DT-Mini-2B, Ocean Optics) were used. This SEC approach was routinely calibrated using standards of known molecular weights, of which the calibration methodology and the relationship between molecular weights and elution volumes were previously described (Wong et al., 2017). We note that the molecular weights reported using this SEC approach are only approximate, as the accuracy of the molecular weight calibration depends on whether the molecular densities of calibration standards are representative of that of WS BrC molecules, which are currently unknown. The absorbance of the different molecular weight fractions were determined by integrating the absorbance of a specific wavelength over the period of elution that corresponds to the molecular weight fraction ($P_{MW,\lambda}$). Since the coupling of the chromatographic technique to UV-VIS absorption measurements leads to the dilution of the BrC sample due to the use of the mobile phase, the absorbance of the molecular weight separated BrC ($A_{BrC,\lambda}$) is related to absorbance of the injected BrC by accounting for the mobile phase flow rate (f) and the volume of the injected BrC sample (V_{BrC}) using Eq. (1) :

$$A_{BrC,\lambda} = \frac{P_{MW,\lambda} \cdot f}{V_{BrC}} \quad (1)$$

The measured light absorption for both bulk WS BrC were normalized by the WSOC concentration of the BrC extract to represent the light absorption per water-soluble organic carbon, or mass absorption coefficient (MAC) of the WS-BrC (the calculation method described in Wong et al., 2017).

Deleted: The molecular weight distributions of WS BrC were determined using high-performance liquid chromatography (HPL GP40 Dionex), equipped with a size exclusion chromatography (SEC)

2.2 Field Observations on Crete Island

2.2.1. Sampling Site and Identification of Biomass Burning Events

Filter samples containing ambient BrC from biomass burning emissions were collected during the fire season (July to October) of 2016 and 2017 at the Heraklion station on Crete, Greece (Figure 1). During the fire season, persistent northerly winds (the Etesians) move air masses across the Aegean Sea, where no further contribution from fire emissions can occur, transporting biomass burning emissions from continental Eastern Europe towards the sampling site. The fire season in 2017 was more intense compared to 2016, due to extended droughts and high temperatures.

Information on location and date of fire events, along with fire radiative power were obtained from the Fire Information for Resource Management System (FIRES, http://firms.modaps.eosdis.nasa.gov/firemap), which was detected by the Moderate Resolution Imaging Spectroradiometer (MODIS). Fire radiative power (in megawatts) was used as a rough proxy for biomass burning emission rate (Wooster, 2002). Fires occurring 3 days prior and within each filter sampling period, with fire radiative power over 100 megawatts, were included in the analysis. Airmass back trajectories were computed via HYSPLIT (Stein et al., 2015), using archived Global Dara Assimilation System (GDAS) meteorology, from which the vertical velocity was determined. New trajectories were computed every hour of each filter sampling interval (i.e., 22 – 24 hours), for a total run time of 72 hours. The information from FIRES and back trajectories were used together to identify filters samples were influenced by fire events (i.e., intersection of back trajectories with the fire locations) and to estimate the corresponding atmospheric transport time from the fire location to the sampling site (example is shown in Figure S3). This analysis approach was chosen to explore the stability of biomass burning tracers, however, it does not account for variability in BrC emissions from various fires. Out of 65 field filter samples collected in the 2016 and 2017 fire seasons (method discussed below), 24 biomass burning filter samples of various atmospheric transport times were identified. We focus our following analysis on these identified biomass burning events, shown in Figure 1. Note that several fires occurring near Athens and on Chios Island were burn events that persisted for multiple days.

2.2.2 Filter Collection, Extraction and Analysis

Ambient BrC in $PM_{2.5}$ were collected on pre-baked 8 × 10 in. quartz filters (2500QAT-UP, Pall) using a high-volume (Hi-Vol) sampler (TISCH) for 22 – 24 hours at a flow rate of 1.4 and 2 m^3 min^{-1} for 2016 and 2017, respectively. Immediately after collection, the filter samples were wrapped in prebaked aluminium foil and stored at -10°C until analysis. In addition, multiple field blanks were collected during both fire seasons. Each quartz filter sample was divided into portions for the determination of various chemical properties. A 1.5 cm^2 punch of the filter sample was analyzed for organic carbon (OC) and elemental carbon using an OCEC Analyzer (Sunset Laboratory Inc) using the NIOSH Method. Another 1.5 cm^2 filter punch was used to determine water-soluble components after extraction by sonication. This included analysis of carbohydrates (levoglucosan, mannosan, galactosan, glucose, mannose, and galactose) using high performance anion exchange chromatography with pulsed amperometric detection (HPAEC-PAD; ICS-3000, Dionex), which is described in Fourtzio et al.

Deleted: Online black carbon absorption measurements were conducted during the fire season of 2017, using a seven wavelen aethalometer (AE31, Magee Scientific).

(2017). Using a separate ion chromatographic system (Dionex), analysis of anions (Cl^-, Br^-, NO_3^-, SO_4^{2-}, $C_2O_4^{2-}$; CS12A column with CERS 500 suppressor) and cations (K^+, Na^+, Ca^{2+}, Mg^{2+}, NH_4^+; AS4A-SC column with AERS 500 suppressor) was also conducted. Potassium associated with biomass burning (i.e., non-sea salt K^+) was determined from the total potassium minus potassium associated with sea-salt. This was calculated using the measured Na^+ concentrations and a standard seawater K^+-to-Na^+ mass ratio of 0.0359 (Seinfeld and Pandis, 1998).

Two 1.5 cm^2 punches were placed in a pre-cleaned 2mL borosilicate glass vial where either 1 mL of purified water (18.2 mΩ) or methanol (MeOH; HPLC grade, Merck) was added and sonicated for 1 hour to extract either the water soluble (WS) or MeOH soluble (i.e., water-soluble and water-insoluble) BrC, respectively. Note that the extractions of MeOH BrC and WS BrC were done on separate sections of the same filter. Each extract was then filtered using a new 0.2 µm PTFE syringe filter (Fisher). For WS BrC, an aliquot of the filtered extract was used to determine the water-soluble organic carbon (WSOC) concentration using the TOC instrument discussed in Section. 2.1.4. For both WS- and MeOH BrC filtered extracts, aliquots of the solutions were used to determine the molecular weight distributions of BrC, using the HPLC-SEC-UV/VIS absorption technique discussed in Section 2.1.4. Additionally, an aliquot of both filtered solutions was used to measure the bulk light absorption properties (i.e., not molecular weight separated) of WS and MeOH BrC, using the absorption spectrometer described in Section 2.1.4. The MAC of the WS and MeOH soluble BrC were determined through normalizing by the WSOC concentration (WS BrC/WSOC) or OC concentrations (MeOH BrC/OC), as determined using the TOC and OCEC analyzers, respectively. Note that for both TOC and bulk UV/VIS absorption measurements, the filtered extracts were diluted by a factor of 20 to ensure the measured properties were in the linear response range of the instruments. The field filter blanks were analysed using the same methodology as the BBOA filters and all measurements were blank subtracted.

3 Results and Discussion

3.1 Laboratory Experiments on WS BrC

3.1.1 Bulk WS BrC

Upon illumination by UVB lights, losses in WSOC were observed for both direct UVB photolysis and UVB + H_2O_2 experiments (Figure 2a), with the majority of this loss occurring following 20 hours of illumination. The effects of aqueous OH oxidation is taken to be the difference between the UVB and UVB + H_2O_2 experiments, assuming that the effects of direct UVB photolysis are identical in both types of experiments (i.e., the addition of H_2O_2 did not significantly alter the rate of direct photolysis). Here, aqueous OH oxidation did not lead to additional loss of WSOC, indicating that the loss of WSOC is only due to direct UVB photolysis.

The effects of photochemical aging on the light absorption per water-soluble organic carbon (mass absorption coefficient, MAC) of WS BrC are shown on Figure 2b. The calculation method for the MAC at 365 and 400 nm is discussed previously in Wong et al. (2017). Note that these MAC values arise from light absorption measurements of water-extracted BrC and not of suspended BrC particles. Initial increase in MAC values was observed due to photochemical aging, suggesting

Deleted: ere

Deleted: , as shown in the blue and green traces of Figure 2a.

Deleted: t

Deleted: ,

Deleted: were

that the WS BrC undergo photoenhancement, leading to increased absorptivity of radiation at 365 and 400 nm, where the increase in MAC values at 365 nm was more significant compared to that at 400 nm. Given that a loss in WSOC was observed during this photoenhancement period, the increased MAC values may be driven by a loss in non-absorbing WSOC and/or the formation of more absorbing WS BrC. This initial increase in MAC values is likely driven by the formation of more absorbing WS BrC, as MAC values increased by a factor of ~ 2 while WSOC decreased only by factor of less than 1.1. During this initial period of photochemical aging (up to 10 hours), the changes in WSOC and MAC_{365} are similar for UVB and UVB + H_2O_2 experiments, suggesting that the aging by UVB led to the observed photoenhancement. Following this period of initial photoenhancement (up to 12 hours), photobleaching (i.e., decrease in MAC values) of WS BrC was observed. Here, a steeper slope for the decrease in MAC values was observed for the UVB + H_2O_2 compared to the UVB experiments, indicating that aqueous OH oxidation leads to enhanced decay in light absorptivity, and that while BrC are susceptible to both degradation due to UVB photolysis and OH oxidation, certain BrC chromophores are more reactive towards OH radicals. Previous studies that have examined the photochemical aging of model biomass burning aromatic compounds (Gelencsér et al., 2003; Chang and Thompson, 2010; Ofner et al., 2011; Zhao et al., 2015; Smith et al., 2016; Hems and Abbatt, 2018), surrogate mixtures of biomass burning BrC (Schnitzler and Abbatt, 2018), and BrC emitted from the pyrolysis of various types of biomass (Zhao et al., 2015; Wong et al., 2017; Sumlin et al., 2017) have similarly observed initial photoenhancement, followed by photobleaching. It has been proposed that polymerization/functionalization of BrC leads to photoenhancement, while fragmentation results in photobleaching.

Deleted: .

Deleted: The

Deleted: were

3.1.2 WS BrC separated by Molecular Weight

Molecular weight separated BrC measurements by SEC provide additional insight into the reactivity of specific classes of WS BrC molecules leading to the observed bulk photoenhancement and photobleaching. This is illustrated in Figure 3 and Figure 4, where the Abs_{365} measurements were binned according to elution volumes, where the high-molecular weight fraction (high-MW) is defined as the sum of light absorptivity (Abs_{365}) for molecules with approximate molecular weights between 66K Da and 401 Da (i.e., elution volumes between 8 and 15 mL) and low molecular weight fraction (low-MW) as the sum of light absorptivity (Abs_{365}) for molecules with approximate molecular weights of 400 Da and less (i.e., elution volumes higher than 15 mL). Prior to photochemical aging, fresh WS BrC consisted of both high- and low-MW chromophores (Figure 3a), however, the contribution of these two fractions to light absorption change when photochemically aged. Figure 4 shows that both molecular weight fractions exhibit dynamic changes in their light absorptivity due to photochemical aging, but to a different extent. High-MW WS BrC undergo substantial intial photoenhancement, followed by photobleaching. Low-MW WS BrC initially decayed within the first hour, then there was an increase in light absorptivity between 1 and 5 hours of illumination time, followed by another period of decreasing light absorptivity. The two separate phases of decreasing light absorptivity suggest that low-MW WS BrC contains chromophores of different photoreactivity. While the photobleaching of both molecular weight fractions appeared largely to follow pseudo first-order kinetics, the photoenhancement of high-MW WS BrC exhibited non-first order behavior. This may be due to the presence of chromophores with different reactivity, or that

after the initial period of photoenhancement, further aging do not lead to further increases in light absorptivity. For simplicity, we treat this period of photoenhancement as pseudo first-order. In order to isolate the effects of OH oxidation on light absorptivity, we follow the approach used by Zhao et al. (2015), where the pseudo first-order OH oxidation rate constants (k^I_{OH}) of photoenhancement/photobleaching were calculated by taking the difference between the observed first-order growth/decay rate constants due to UVB photolysis (k^I_{UVB}) and UVB + H_2O_2 photolysis experiments ($k^I_{UVB+H2O2}$), using Eq. (2). The second-order OH oxidation rate constant (k^{II}_{OH}) can be calculated from Eq. (3).

$$k^I_{OH} = k^I_{UVB+H2O2} - k^I_{UVB} \quad (2)$$

$$k^{II}_{OH} = k^I_{OH} / [OH]_{ss} \quad (3)$$

We note that for Eq. (2), $[OH]_{ss}$ represents the steady state conentration of OH radicals due to the photolysis of 1.5 mM of H_2O_2 (i.e., difference in $[OH]_{ss}$ between UVB photolysis and UVB+ H_2O_2 photolysis experiments). Additionally, for the high-MW BrC, the photoenhancement and photobleaching rate constants were determined by fitting first-order curves to the first 3 hours and between 8 and 18 hours of absorption data at 365nm (Figure S4a). For the low-MW WS BrC, to determine the decay rate constants of rapidly and slowly photobleached chromophores, a first-order decay curve was fitted to 0 to 1 hours and 8 to 18 hours of absorption data at 365 nm, respectively (Figure S4b).

The resulting observed rate constants for photoenhancement and photobleaching due to aqueous OH oxidation and UVB photolysis are shown in Table 1. Here, the corresponding rate constants due to UVA photolysis, which were determined by our previous work (Wong et al., 2017) are included for comparison. Considering the reaction rate constants for low-MW WS BrC, their inital photoenhancement was only observed in the presence of UVA radiation (i.e., enhanced photon flux at wavelengths above 310 nm), indicating reactions leading to the increased light absorptivity are wavelength dependent. Whereas photochemical aging of low-MW WS BrC by UVB photolysis and aqueous OH oxidation only leads to photobleaching. As mentioned previously, low-MW WS BrC of different reactivities with respect to photobleaching by aqueous OH oxidation and UVB photolysis were observed; chromophores that were rapidly photobleached due to exposure to UVB lights and chromophores that were slowly photobleached by both aqueous OH oxidiation and UVB radiation. We note that the second-order rate constant for the decay in light absorptivity due to the OH reaction with slowly photobleached low-MW WS chromophores determined in this study [$(2.9 \pm 0.5) \times 10^9$ M^{-1} s^{-1}] is comparable to the range of the concentration-based rate constants for the OH reaction with 3 different nitrophenols ([$(3.7 - 5.0) \times 10^9$ M^{-1} s^{-1}], as reported by Hems and Abbatt (2017). Given that nitrophenols, a class of WS BrC that have been detected in BBOA in significant concentrations (Mohr et al., 2013; Lin et al., 2016), have molecular weights that are approximately less than 200 Da, it is reasonable that they govern the OH reactivity of low-MW WS BrC (i.e., ≤ 400 Da) observed in this study.

For high-MW WS BrC, no differences in the evolution of their light absorption were observed between the two different photochemical aging experiments (Figure 4a). This suggests that their initial photoenhancement (up to 15 hours), and subsequent photobleaching, were only due to exposure to UVB radiation. Given that the photoenhancement and photobleaching rates for high-MW WS chromophores due to UVB and UVA exposure (Table 1) are similar, and that both UVB and UVA lamps have similar photon fluxes for wavelengths lower than 310nm, our results suggest that most of the

Deleted: 1
Deleted: 2
Deleted: 1
Deleted: k^{II}_{OH} /
Deleted: 2
Deleted: and
Deleted: Considering the evolution of
Deleted: (Figure 4a), at early reaction times, changes
Deleted: absorptivity
Deleted: only
Deleted: due to UVB exposure, where there was only
Deleted: followed by photobleaching

photochemical aging was initiated by UVB radiation. Owing to their rapid photoenhancement and slow photobleaching, the contribution of high-MW WS BrC to total light absorptivity increases throughout photochemical aging, from 20% when the WS BrC was freshly emitted, up to 80% after 100 hours of UV exposure (Figure 4b). Given that the integrated UVB photon flux in these laboratory experiments is roughly 92% of the sun at Solar Noon (i.e., one hour of UVB exposure in laboratory experiments is equivalent to 0.92 hours in the atmosphere), these results further support earlier field observations where the light absorptivity of aged (up to 40 hours) ambient biomass burning WS BrC was attributed to molecules larger than 500 Da (Di Lorenzo and Young, 2016; Di Lorenzo et al., 2017).

Changes in the absorption Angström exponent (AAE) throughout UVB photolysis and OH oxidation were also determined from linear regression fits to logAbs vs. logλ (Figure S5) in the wavelength ranges of 320-500 nm for both high and low-MW fractions of WS BrC molecules, and 320-420 nm for high-MW BrC. Changes in AAE values that were determined from different wavelength ranges can provide insight into the effects of photochemical aging on the light absorption spectral properties of BrC, in addition to monitoring the MAC values at different wavelengths. Shown in Figure 5, prior to any photochemical aging, different AAE values for low-MW (10.0 ± 0.4) and high-MW (6.4 ± 0.7) WS BrC were observed, indicating that the low-MW WS BrC have a much stronger spectral dependence than that of high-MW WS BrC. We speculate that the lower AAE values of high-MW WS BrC are due to the highly conjugated nature of these molecules, as previous observations by Hopkins et al. (2007) have indicated that biomass burning BrC with lower AAE values have a higher extent of carbon sp^2 hybridization compared to those with higher AAE values. As the low- and high-MW WS BrC were photochemically aged, changes in their AAE values were observed. For low-MW WS BrC, AAE values decreased due to decreased light absorptivity at lower wavelengths. For high-MW WS BrC, comparison of the temporal evolution of the AAE values determined in both wavelength ranges (Figure 5b-c) shows that during initial photoenhancement (up to 15 hours), a slight decrease in AAE was only observed from 320-420nm, suggesting that photoenhancement reactions, such as functionalization and polymerization, enhance the absorptivity of light of wavelengths only up to 500 nm. Following this period of initial photoenhancement, increasing AAE values was observed as the high-MW WS BrC was photobleached, where the increase in AAE values for 320-500 nm was more rapid compared to 320-420nm, indicating a blue shift in the absorption spectra of high-MW WS BrC due to decreasing absorption in the 420 to 500 nm range. Collectively, the differences in evolution of AAE values further support that the reactivity and aging mechanisms of BrC are dependent on their molecular weight.

Deleted: This was done to provide additional

Deleted:). Prior

Deleted: were

3.1.3 Atmospheric Fate of WS BrC from Biomass Burning

These experimentally determined rate constants indicate that ambient WS BrC is transformed within a day in the atmosphere (Table S1; calculation method discussed in Section S2), and considering that the average atmospheric lifetime of particles with respect to deposition is approximately one week, our laboratory results indicate that photochemical aging has an important effect on the optical properties of BBOA. For low-MW WS BrC, laboratory results suggest that there are two groups with different reactivities. A highly photolabile fraction of low-MW WS BrC is photobleached in the atmosphere, with UVB photolysis being their dominant atmospheric fate with an estimated atmospheric lifetime of 0.7 ± 0.2 hours. A second, less

Deleted: are

Deleted: b

reactive fraction of low-MW WS BrC has an estimated atmospheric lifetime of 9.8 ± 1.6 hours, with aqueous OH oxidation representing its dominant atmospheric loss mechanism. However, this less reactive low-MW WS BrC does not significantly contribute to total light absorptivity, as their decay only increased the fractional contribution of high-MW to total light absorptivity for WS BrC by 0.2 (Figure 4b). Conversely, for high-MW WS BrC, following their initial photoenhancement where color formation occurs over a timescale of a few hours, these BrC is photobleached by UVB photolysis, with atmospheric lifetime of 11 ± 2.3 hours.

While these estimated atmospheric lifetimes suggest that the majority of BrC is photobleached in the atmosphere, it is important to note that for high-MW WS BrC, the rate of decreasing light absorptivity slows down with time, where after 100 hours of photochemical aging in the laboratory, approximately 20% of the initial light absorptivity remained (Figure 4a). These observations suggest that a fraction of high-MW WS-BrC has an atmospheric lifetime longer than 11 hours and is more persistent. It is critical to note that these atmospheric lifetimes were estimated from laboratory generated BrC from one biomass fuel type, under a specific burn condition. In addition, the estimated atmospheric lifetimes were calculated assuming continuous exposure to solar radiation with an actinic flux corresponding to that at Solar Noon and $[OH]_{ss}$ of 1.0 x 10^{-14} M, which represent the daily peak solar photon flux and the upper range of OH concentrations in cloud droplets (Herrmann et al., 2010; Arakaki et al., 2013), thus likely representing the lower range of BrC atmospheric lifetimes. We also stress that there are uncertainities in these estimates, as they assume that the photolysis quantum yield of BrC is wavelength independent. Also, estimates of $[OH]_{ss}$ in the condensed phase, which includes aqueous particles, cloud and fog droplets, range over several orders of magnitude (Arakaki et al., 2013; Ervens, 2015). Under lower levels of $[OH]_{ss}$, which better represents the oxidant concentrations of aerosol particles, photolysis by UVB becomes the domiant atmospheric loss mechanism for all molecular weight fractions of BrC.

3.2 Field Observations

3.2.1 Bulk and Molecular Weight Separated WS and MeOH BrC

Investigating the impacts of atmospheric aging on biomass burning BrC in the field and comparison to laboratory observations represent the other primary goals of this study. Both WS and MeOH (i.e., water-soluble and insoluble) BrC were analysed for the field samples, to assess the atmospheric evolution of BrC from ambient BBOA. Evolution of various properties of WS and MeOH BrC as a function of atmospheric transport time is shown in Figure 6, where all individuals measurements (filled points), along with binned (every 5 hours) median values (open points) are presented. We first discuss the bulk measurements (Figure 6a-d).

Considering field samples with atmospheric transport times up to 10 hours, an increase in bulk (i.e., not molecular weight separated) Abs_{365nm} (Figure 6b) was observed for both MeOH and WS BrC, while a significant increase in MAC_{365} values (Figure 6c) was only observed for the water-soluble portion. This is due to the more significant loss of WSOC compared to OC (Figure 6a), suggesting that the non-absorbing water-soluble compounds in biomass burning are more rapidly lost in

Deleted: have

Deleted: are

Deleted: are

Deleted: have

Deleted: are

Deleted: We note that

Formatted: Indent: First line: 0.5"

the atmosphere due to aging. For field samples with atmospheric transport times longer than 10 hours, lower values of WSOC, OC, Abs_{365} values for MeOH and WS BrC were observed, suggesting that atmospheric aging processes led to a decay in the mass and light absorptivity of biomass burning BrC. These ambient observations of bulk WS BrC corroborate our earlier laboratory results, suggesting that atmospheric photochemical aging processes increase MAC values for WS BrC, at least in fresher biomass burning plumes, followed by photobleaching with further atmospheric aging. Despite the considerable scatter, the field data indicate that the light absorptivity of bulk MeOH BrC decreased at a slower rate compared to bulk WS BrC (see Figure S6 for exponential decay). From these exponential decays in bulk MeOH and WS ambient BrC, the atmospheric lifetime of bulk MeOH and WS BrC is estimated to be between 15 – 28 hours. We note that within the variability of all ambient observations, the MAC values for MeOH BrC did not change significantly. Lastly, from these bulk measurements, AAE values (Figure 6d) did not change significantly throughout atmospheric transport, suggesting that aging processes do not greatly affect the wavelength dependence of BrC light absorption.

Molecular weight separated BrC measurements from the corresponding field samples (Figure 6e) indicate that even for fresh biomass burning emissions (i.e., one hour of atmospheric transport time), high-MW MeOH and WS BrC dominated the total light absorption at 365 nm. This is also highlighted in Figure 3b, which shows the molecular weight separated absorption spectra of fresh ambient biomass burning WS BrC. Given that it remains unclear to which extent fuel type and burn conditions affect the molecular weight distribution of BrC chromophores, the observed low contribution of low-MW BrC to total light absorptivity may either be due to their rapid photochemical removal in the atmosphere, as demonstrated from our laboratory experiments, or their low emission rate. In addition, the average contribution of high-MW chromophores to total BrC light absorptivity is lower compared to WS BrC, suggesting that some water-insoluble BrC are low-MW compounds.

Given that the atmospheric lifetime of ambient BrC from bulk measurements was estimated to be between 15 – 19 hours, and that high-MW chromophores contributed on average 75-87% of total light absorptivity for MeOH and WS ambient BrC, the atmospheric lifetime of ambient high-MW MeOH and WS BrC is likely to be at least 15 – 28 hours as well, which is longer than the estimates from laboratory results for the WS BrC ($\tau \sim 11 \pm 2.3$ hours, Table S1). We spectulate that the difference in atmospheric lifetime may be due to several reasons. Firstly, the laboratory constrainted atmospheric lifetime represents BrC emitted from the combustion of one biomass fuel type under smoldering conditions, which may not represent ambient fire conditions, as the light absorption properties of BrC have been observed to be dependent on field and burn conditions (Chen and Bond, 2010). Secondly, the laboratory constrained atmospheric lifetime represents high-MW WS BrC that was cloud processed, which may not apply for the ambient samples. Thirdly, high-MW WS BrC was continuously exposed to UV radiation in the laboratory, where this does not represent the dinural cycle of solar radiation ambient BrC is exposed to. This is particularly important for high-MW WS BrC emitted throughout the night, where its atmospheric lifetime will be longer relative to that emitted during the day, during which the high-MW WS BrC is photobleached. Fourthly, the lifetime obtrained from laboratory results were based on the aging of BrC dissolved in bulk solutions, where parameters that may affect the reactivity of ambient BrC in suspended particles, such as aerosol phase state, solute concentrations, and viscosity were not accounted for. Similarly, ambient aerosols containing biomass burning BrC are likely to be more chemically complex than

Deleted: 19 hours.

Deleted: We note that while black carbon mass concentrations were only measured at the field site during the 2017 fire season, AAE values were observed to be inversely proportional to the bla carbon to organic aerosol ratios (Figure S7), further extending previous demonstrations of this relationship from laboratory-generated and ambient biomass burning BrC (Saleh et al., 2014; et al., 2015; Gilardoni et al., 2016; Costabile et al., 2017)

Deleted: estimated

Deleted: 19

Deleted: high-MW WS BrC that were cloud processed, which not apply for the ambient samples. Secondly

Deleted: were

Deleted: those

Deleted: are

Deleted: Thirdly

Deleted: aeorsols

those studied in the laboratory (e.g., complex emissions from the combustion of multiple types of biomass), where the presence of other organic compounds that are more reactive may prolong the atmospheric lifetime of ambient high-MW BrC. Lastly, there may be uncertainties associated with the estimated atmospheric transport times for field samples, either due to unaccounted contributions from a) fires occuring more than 3 days prior to filter collection (i.e., HYSPLIT runs times of 72 hours were used) or b) small fires with fire radiative power less than 100 MW, which were not included in the current analysis, or c) large fires that are not detected by MODIS due to interference effects by thick smoke (Schroeder et al., 2008).

3.2.2 Chemical Tracers for Aged BrC from Biomass Burning

Previous studies have suggested the limitations of using levoglucosan and non-sea salt potassium (nss-K^+) as chemical tracers for biomass burning, due to levoglucosan's short atmospheric lifetime (e.g., Hennigan et al., 2010; May et al., 2012) and emission of nss-K^+ by non-biomass burning sources (Urban et al., 2012). More recently, Scaramboni et al. (2015), suggested the use of total hydrous sugars (e.g., glucose) as an alternative tracer for biomass burning, since the six-membered ring of hydrated sugar molecule is potentially more stable than the five-membered ring of levoglucosan. While biological aerosols, such as microbes, are also a source of hydrated sugars (Graham et al., 2002) and may interfere with the signal from biomass burning, it is still useful to examine correlations of these types of sugars with BrC under known periods of biomass burning influence - especially given that high-MW BrC from biomass burning appears to be a relatively stable aerosol component, such that it can still be observed after significant periods of aging.

Focusing on the ambient filter samples impacted by biomass burning with estimated atmospheric transport times over 10 hours, we compare correlations of levoglucosan, nss-K^+, and total hydrous sugars (defined as the sum of glucose, mannose, and galactose mass concentration) to BrC, to assess how these compounds compare to BrC as a biomass burning tracer for aged BBOA. Figure 7 shows their correlations to MeOH and WS BrC light absorption at 365 nm. The detailed results of these regression analyses are provided in Table S2. No correlation is seen between levoglucosan and aged MeOH and WS BrC ($r^2 \leq 0.01$), suggesting that levoglucosan is not likely to be representative of absorbing organic components, nor serve as an effective tracer of aged biomass burning. Given that we did not account for the fire conditions in this analysis, the lack of correlation can also arise due to varying relative emission ratios of BrC to levoglucosan, since it has been previously observed that the relative emission ratios of OA to levoglucosan and BrC to OA are not constant across burning conditions (i.e., smoldering vs. flaming) (Mazzoleni et al., 2007; Kalogridis et al., 2018). In comparison, both WS and total BrC correlated moderately with nss-K^+ ($0.50 \leq r^2 \leq 0.70$), consistent with previous field measurements of BBOA from the boreal forest (Di Lorenzo et al., 2018) and Amazon rainforest (Fuzzi et al., 2007). The moderate correlations may potentially be due to differences in the dependence of potassium emissions and BrC light absorptivity on fire conditions (Chen and Bond, 2010; Lee et al., 2010). Additionally, contributions of nss-K^+ from other non-biomass burning sources, such as crustal material, could also diminish the correlation with BrC if BrC is more specific to biomass burning than nss-K^+. Moderate to strong correlations between light absorptivity of (MeOH and WS) BrC and total hydrous sugars were observed ($0.56 \leq r^2 \leq 0.83$), suggesting that both class of compounds may serve as a robust tracer for aged biomass burning emissions.

Deleted: i

Deleted: reported

Deleted: a

Deleted: with

Deleted: to

Deleted: how they compare to BrC as a biomass burning trace for aged BBOA. Figure 7 shows their correlations to MeOH and BrC light absorption at 365 nm. The detailed results of these regression analysis are provided in Table S2. No correlation is se between levoglucosan and aged MeOH and WS BrC ($r^2 \leq 0.01$), suggesting that levoglucosan is not likely to be representative of absorbing organic components, nor serve as an effective tracer o aged biomass burning.

4. Conclusions and Atmospheric Implications

In this work, the effects of atmospheric aging on the light absorptivity of molecular weight separated-BrC were demonstrated in both controlled laboratory experiments and ambient observations. The laboratory work focused on the aging of WS BrC and the experimental conditions most likely represent cloud processing of BBOA. The ambient data included analysis of both WS and MeOH BrC. In the laboratory experiments, photochemical aging processes led to significant changes in light absorptivity and molecular weight distributions of BrC, where the reactivity of WS BrC was observed to be dependent on molecular weight. We found that low-MW WS BrC undergoes rapid photobleaching in the atmosphere on timescales of a few hours, whereas high-MW WS BrC likely persist in the atmopshere up to a few days. These laboratory results bridge contrasting results from previous laboratory and field observations that show low-MW WS BrC, such as nitrophenols, were rapidly photobleached within several hours, while high-MW WS BrC are more stable. Ambient BrC was largely composed of WS BrC species, and for both WS and MeOH BrC, their light absorptivity was dominated by high-MW BrC, consistent with our laboratory results. Ambient BrC was observed to undergo initial photoenhancement and high-MW BrC dominated total light absorption at 365nm, even for fresh (~1 hour of atmospheric transport) biomass burning emissions, further supporting that low-MW BrC is a short lived component in atmospheric BBOA. Additionally, observations of initial photoenhancement due to atmospheric aging in both laboratory and field data support earlier ambient observations that secondary production of BrC from biomass burning emissions can be an important source of light absorbing aerosol (Gilardoni et al., 2016), but only near fire emissions. From the observed decay of bulk WS light absorptivity, we estimate that ambient WS BrC have atmospheric lifetimes of approximately 15 - 28 hours. This range of atmospheric lifetime likely corresponds to that of high-MW BrC, as it contributed over 75% to total light absorptivity of ambient BrC of ages up to 68 hours. It is important to note that while this estimated atmospheric lifetime likely represents a majority of high-MW BrC, the slope of the light absorptivity decay curve (Figure S6) decreased with atmospheric age, indicating that a fraction of the high-MW BrC is persistent in the atmosphere, for at least up to 68 hours. Collectively, this field-constrained lifetime of high-MW WS BrC is much larger than that obtained from laboratory results, which may be due to differences in the assumed versus ambient solar photon fluxes and oxidant concentrations. In addition, aging processes not investigated in the laboratory study, such as dilution, are also unlikely to result in more rapid removal of high-MW BrC from the atmosphere. Although the volatility of high-MW BrC compounds remains uncharacterized, given their large molecular weights and solubility in water, we expect them to exhibit very low volatility and are unlikely to be lost from biomass burning particles via volatilization during dilution with background airmasses, which is consistent with the observation that the majority of wood smoke BrC is associated with extremely low-volatility organic compounds (Saleh et al., 2014).

Given that the average lifetime of particles in the atmosphere is approximately one week with respect to deposition, the estimated atmospheric lifetime of high-MW BrC continues to support earlier observations that it can be persistent component in atmospheric BBOA (Di Lorenzo and Young, 2016; Wong et al., 2017; Di Lorenzo et al., 2017) and therefore has a larger impact on aerosol direct radiative forcing compared to low-MW BrC. The stability of high-MW BrC also suggests that it may be ubiquitous in the atmosphere and potentially undergo intercontinental transport. In addition, the estimated

Deleted: s

Deleted: are

Deleted: s

Deleted: 19

Deleted: they

Deleted: t

Deleted: are

Deleted: .

Deleted: they

Deleted: s

Deleted: have

Deleted: they

atmospheric lifetimes of ambient BrC from this study (15 – 28 hours) are consistent to those from previous field studies of wildfires in Northwest USA (τ: 13 - 22 hours; Forrister et al., 2015) and in the Amazon (τ: 22 - 45 hours; Wang et al., 2016). A recent modelling study indicated that incorporating a 1-day photobleaching e-folding time, which was constrained from these previous field studies, improved modelled-vs-observed BrC absorption and decreased the estimated positive direct radiative effect of organic aerosols (Wang et al., 2018). Further field data from different geographical regions are necessary to assess the estimated 1-day BrC atmospheric lifetime and to improve predictions of global BrC impacts.

Accurate predictions of the direct radiative forcing also require robust estimates of the contribution of biomass burning to global BrC. Our field observations suggest total hydrous sugars and BrC may be more robust biomass burning markers compared to levoglucosan and nss-K^+. Other potential sources of hydrous sugars should also be assessed to better constrain their use as tracers for biomass burning.

From our field observations, the fractional contribution of high-MW MeOH and WS BrC to total (all molecular weights) light absorptivity remained relatively constant up to 68 hours of atmospheric aging, suggesting that this class of compounds may also provide an alternative marker for aged biomass burning emissions. However, it remains unclear whether fuel type and burn conditions influence the emission, chemical composition, and reactivity of high-MW BrC. For example, while the absorptivity of MeOH and WS BrC generated from wood smoke has been shown to be dependent on pyrolysis temperature and wood types (Chen and Bond, 2010), it remains unclear whether this is due to differences in the emission of low or high-MW BrC. Characterization of high-MW BrC generated from other commonly burned biomass, such as agriculture crop residues and biofuels used for residental heating, under representative combustion and fuel conditions (dry or wet), is warranted.

Data Availability: SEC data can be requested from the corresponding author. All other data are uploaded and available at https://doi.pangaea.de/10.1594/PANGAEA.896731

Author Contribution: JPSW, AN, and RJW designed the laboratory experiment. JPSW performed laboratory experiments and analyzed the data. NM, KV, MK, JS, AN designed and organized the field campaign. MT and IT collected the field samples and conducted the OC/EC and ion chromatrography measurements. JS carried out the carbohydrate analysis. JPSW conducted and analyzed light absorption and WSOC measurements for field samples. JPSW wrote the manuscript with contributions from AN and RJW. All authors commented on the final manuscript.

Acknowledgements. This work was supported by Electric Power Research Institute (EPRI) through contract #00-10003806 and NASA throguh constract NNX14A974G, and from the project PyroTRACH (ERC-2016-COG) funded from H2020-EU.1.1. - Excellent Science - European Research Council (ERC), project ID 726165.

Deleted: 19

Deleted: ese

Deleted: ry

Deleted: . Athanasios Nenes acknowledges support from the

Deleted: Project PyroTRACH (Pyrogenic TRansformation Affecting Climate and Health) grant agreement

References

Alexander, D. T. L., Crozier, P. A. and Anderson, J. R.: Brown Carbon Spheres in East Asian Outflow and Their Optical Properties, Science, 321(5890), 833–836, doi:10.1126/science.1155296, 2008.

Anastasio, C. and McGregor, K. G.: Chemistry of fog waters in California's Central Valley: 1. In situ photoformation of hydroxyl radical and singlet molecular oxygen, Atmos. Environ., 35(6), 1079–1089, doi:10.1016/S1352-2310(00)00281-8, 2001.

Andreae, M. O. and Gelencsér, A.: Black carbon or brown carbon? The nature of light-absorbing carbonaceous aerosols, Atmos. Chem. Phys., 6(10), 3131–3148, doi:10.5194/acp-6-3131-2006, 2006.

Arakaki, T., Anastasio, C., Kuroki, Y., Nakajima, H., Okada, K., Kotani, Y., Handa, D., Azechi, S., Kimura, T., Tsuhako, A. and Miyagi, Y.: A General Scavenging Rate Constant for Reaction of Hydroxyl Radical with Organic Carbon in Atmospheric Waters, Environ. Sci. Technol., 47(15), 8196–8203, doi:10.1021/es401927b, 2013.

Badali, K. M., Zhou, S., Aljawhary, D., Antiñolo, M., Chen, W. J., Lok, A., Mungall, E., Wong, J. P. S., Zhao, R. and Abbatt, J. P. D.: Formation of hydroxyl radicals from photolysis of secondary organic aerosol material, Atmos. Chem. Phys., 15(14), 7831–7840, doi:10.5194/acp-15-7831-2015, 2015.

Bond, T. C.: Spectral dependence of visible light absorption by carbonaceous particles emitted from coal combustion, Geophys. Res. Lett., 28(21), 4075–4078, doi:10.1029/2001GL013652, 2001.

Bougiatioti, A., Stavroulas, I., Kostenidou, E., Zarmpas, P., Theodosi, C., Kouvarakis, G., Canonaco, F., Prévôt, A. S. H., Nenes, A., Pandis, S. N. and Mihalopoulos, N.: Processing of biomass-burning aerosol in the eastern Mediterranean during summertime, Atmos. Chem. Phys., 14(9), 4793–4807, doi:10.5194/acp-14-4793-2014, 2014.

Chang, J. L. and Thompson, J. E.: Characterization of colored products formed during irradiation of aqueous solutions containing H2O2 and phenolic compounds, Atmos. Environ., 44(4), 541–551, doi:10.1016/j.atmosenv.2009.10.042, 2010.

Chen, Y. and Bond, T. C.: Light absorption by organic carbon from wood combustion, Atmos. Chem. Phys., 10(4), 1773–1787, doi:10.5194/acp-10-1773-2010, 2010.

Desyaterik, Y., Sun, Y., Shen, X., Lee, T., Wang, X., Wang, T. and Collett, J. L.: Speciation of "brown" carbon in cloud water impacted by agricultural biomass burning in eastern China, J. Geophys. Res. Atmospheres, 118(13), 7389–7399, doi:10.1002/jgrd.50561, 2013.

Di Lorenzo, R. A. and Young, C. J.: Size separation method for absorption characterization in brown carbon: Application to an aged biomass burning sample, Geophys. Res. Lett., 43(1), 2015GL066954, doi:10.1002/2015GL066954, 2016.

Di Lorenzo, R. A., Washenfelder, R. A., Attwood, A. R., Guo, H., Xu, L., Ng, N. L., Weber, R. J., Baumann, K., Edgerton, E. and Young, C. J.: Molecular-Size-Separated Brown Carbon Absorption for Biomass-Burning Aerosol at Multiple Field Sites, Environ. Sci. Technol., 51(6), 3128–3137, doi:10.1021/acs.est.6b06160, 2017.

Di Lorenzo, R. A., Place, B. K., VandenBoer, T. C. and Young, C. J.: Composition of Size-Resolved Aged Boreal Fire Aerosols: Brown Carbon, Biomass Burning Tracers, and Reduced Nitrogen, ACS Earth Space Chem., doi:10.1021/acsearthspacechem.7b00137, 2018.

Deleted: Costabile, F., Gilardoni, S., Barnaba, F., Di Ianni, A., Liberto, L., Dionisi, D., Manigrasso, M., Paglione, M., Poluzzi, V Rinaldi, M., Facchini, M. C. and Gobbi, G. P.: Characteristics of brown carbon in the urban Po Valley atmosphere, Atmos. Chem. Phys., 17(1), 313–326, doi:10.5194/acp-17-313-2017, 2017.¶

Dinar, E., Riziq, A. A., Spindler, C., Erlick, C., Kiss, G. and Rudich, Y.: The complex refractive index of atmospheric and model humic-like substances (HULIS) retrieved by a cavity ring down aerosol spectrometer (CRD-AS), Faraday Discuss., 137(0), 279–295, doi:10.1039/B703111D, 2008.

Ervens, B.: Modeling the Processing of Aerosol and Trace Gases in Clouds and Fogs, Chem. Rev., 115(10), 4157–4198, doi:10.1021/cr5005887, 2015.

Fan, X., Wei, S., Zhu, M., Song, J. and Peng, P.: Comprehensive characterization of humic-like substances in smoke PM2.5 emitted from the combustion of biomass materials and fossil fuels, Atmos. Chem. Phys., 16(20), 13321–13340, doi:10.5194/acp-16-13321-2016, 2016.

Feng, Y., Ramanathan, V. and Kotamarthi, V. R.: Brown carbon: a significant atmospheric absorber of solar radiation?, Atmos. Chem. Phys., 13(17), 8607–8621, doi:10.5194/acp-13-8607-2013, 2013.

Forrister, H., Liu, J., Scheuer, E., Dibb, J., Ziemba, L., Thornhill, K. L., Anderson, B., Diskin, G., Perring, A. E., Schwarz, J. P., Campuzano-Jost, P., Day, D. A., Palm, B. B., Jimenez, J. L., Nenes, A. and Weber, R. J.: Evolution of brown carbon in wildfire plumes: Brown Carbon in Biomass Burning Plumes, Geophys. Res. Lett., 42(11), 4623–4630, doi:10.1002/2015GL063897, 2015.

Fourtziou, L., Liakakou, E., Stavroulas, I., Theodosi, C., Zarmpas, P., Psiloglou, B., Sciare, J., Maggos, T., Bairachtari, K., Bougiatioti, A., Gerasopoulos, E., Sarda-Estève, R., Bonnaire, N. and Mihalopoulos, N.: Multi-tracer approach to characterize domestic wood burning in Athens (Greece) during wintertime, Atmos. Environ., 148, 89–101, doi:10.1016/j.atmosenv.2016.10.011, 2017.

Fuzzi, S., Decesari, S., Facchini, M. C., Cavalli, F., Emblico, L., Mircea, M., Andreae, M. O., Trebs, I., Hoffer, A., Guyon, P., Artaxo, P., Rizzo, L. V., Lara, L. L., Pauliquevis, T., Maenhaut, W., Raes, N., Chi, X., Mayol-Bracero, O. L., Soto-García, L. L., Claeys, M., Kourtchev, I., Rissler, J., Swietlicki, E., Tagliavini, E., Schkolnik, G., Falkovich, A. H., Rudich, Y., Fisch, G. and Gatti, L. V.: Overview of the inorganic and organic composition of size-segregated aerosol in Rondônia, Brazil, from the biomass-burning period to the onset of the wet season, J. Geophys. Res. Atmospheres, 112(D1), doi:10.1029/2005JD006741, 2007.

Gelencsér, A., Hoffer, A., Kiss, G., Tombácz, E., Kurdi, R. and Bencze, L.: In-situ Formation of Light-Absorbing Organic Matter in Cloud Water, J. Atmospheric Chem., 45(1), 25–33, doi:10.1023/A:1024060428172, 2003.

Gilardoni, S., Massoli, P., Paglione, M., Giulianelli, L., Carbone, C., Rinaldi, M., Decesari, S., Sandrini, S., Costabile, F., Gobbi, G. P., Pietrogrande, M. C., Visentin, M., Scotto, F., Fuzzi, S. and Facchini, M. C.: Direct observation of aqueous secondary organic aerosol from biomass-burning emissions, Proc. Natl. Acad. Sci., 113(36), 10013–10018, doi:10.1073/pnas.1602212113, 2016.

Graham, B., Mayol-Bracero, O. L., Guyon, P., Roberts, G. C., Decesari, S., Facchini, M. C., Artaxo, P., Maenhaut, W., Köll, P. and Andreae, M. O.: Water-soluble organic compounds in biomass burning aerosols over Amazonia 1. Characterization by NMR and GC-MS, J. Geophys. Res. Atmospheres, 107(D20), LBA 14-1-LBA 14-16, doi:10.1029/2001JD000336, 2002.

He, S. and Carmichael, G. R.: Sensitivity of photolysis rates and ozone production in the troposphere to aerosol properties, J. Geophys. Res. Atmospheres, 104(D21), 26307–26324, doi:10.1029/1999JD900789, 1999.

Hecobian, A., Zhang, X., Zheng, M., Frank, N., Edgerton, E. S. and Weber, R. J.: Water-Soluble Organic Aerosol material and the light-absorption characteristics of aqueous extracts measured over the Southeastern United States, Atmos. Chem. Phys., 10(13), 5965–5977, doi:10.5194/acp-10-5965-2010, 2010.

Hems, R. F. and Abbatt, J. P. D.: Aqueous Phase Photo-oxidation of Brown Carbon Nitrophenols: Reaction Kinetics, Mechanism, and Evolution of Light Absorption, ACS Earth Space Chem., doi:10.1021/acsearthspacechem.7b00123, 2018.

Hennigan, C. J., Sullivan, A. P., Collett, J. L. and Robinson, A. L.: Levoglucosan stability in biomass burning particles exposed to hydroxyl radicals, Geophys. Res. Lett., 37(9), L09806, doi:10.1029/2010GL043088, 2010.

Herrmann, H., Hoffmann, D., Schaefer, T., Bräuer, P. and Tilgner, A.: Tropospheric Aqueous-Phase Free-Radical Chemistry: Radical Sources, Spectra, Reaction Kinetics and Prediction Tools, Chem. Phys. Chem., 11(18), 3796–3822, doi:10.1002/cphc.201000533, 2010.

Hoffer, A., Gelencsér, A., Guyon, P., Kiss, G., Schmid, O., Frank, G. P., Artaxo, P. and Andreae, M. O.: Optical properties of humic-like substances (HULIS) in biomass-burning aerosols, Atmos. Chem. Phys., 6(11), 3563–3570, doi:10.5194/acp-6-3563-2006, 2006.

Hoffmann, D., Tilgner, A., Iinuma, Y. and Herrmann, H.: Atmospheric Stability of Levoglucosan: A Detailed Laboratory and Modeling Study, Environ. Sci. Technol., 44(2), 694–699, doi:10.1021/es902476f, 2010.

Hopkins, R. J., Lewis, K., Desyaterik, Y., Wang, Z., Tivanski, A. V., Arnott, W. P., Laskin, A. and Gilles, M. K.: Correlations between optical, chemical and physical properties of biomass burn aerosols, Geophys. Res. Lett., 34(18), doi:10.1029/2007GL030502, 2007.

Jo, D. S., Park, R. J., Lee, S., Kim, S.-W. and Zhang, X.: A global simulation of brown carbon: implications for photochemistry and direct radiative effect, Atmos. Chem. Phys., 16(5), 3413–3432, doi:10.5194/acp-16-3413-2016, 2016.

Kalogridis, A.-C., Popovicheva, O. B., Engling, G., Diapouli, E., Kawamura, K., Tachibana, E., Ono, K., Kozlov, V. S. and Eleftheriadis, K.: Smoke aerosol chemistry and aging of Siberian biomass burning emissions in a large aerosol chamber, Atmos. Environ., 185, 15–28, doi:10.1016/j.atmosenv.2018.04.033, 2018.

Kessler, S. H., Smith, J. D., Che, D. L., Worsnop, D. R., Wilson, K. R. and Kroll, J. H.: Chemical Sinks of Organic Aerosol: Kinetics and Products of the Heterogeneous Oxidation of Erythritol and Levoglucosan, Environ. Sci. Technol., 44(18), 7005–7010, doi:10.1021/es101465m, 2010.

Kirchstetter, T. W. and Thatcher, T. L.: Contribution of organic carbon to wood smoke particulate matter absorption of solar radiation, Atmos. Chem. Phys., 12(14), 6067–6072, doi:10.5194/acp-12-6067-2012, 2012.

Lack, D. A., Langridge, J. M., Bahreini, R., Cappa, C. D., Middlebrook, A. M. and Schwarz, J. P.: Brown carbon and internal mixing in biomass burning particles, Proc. Natl. Acad. Sci., 109(37), 14802–14807, doi:10.1073/pnas.1206575109, 2012.

Laskin, A., Laskin, J. and Nizkorodov, S. A.: Chemistry of Atmospheric Brown Carbon, Chem. Rev., 115(10), 4335–4382, doi:10.1021/cr5006167, 2015.

Lee, T., Sullivan, A. P., Mack, L., Jimenez, J. L., Kreidenweis, S. M., Onasch, T. B., Worsnop, D. R., Malm, W., Wold, C. E., Hao, W. M. and Jr, J. L. C.: Chemical Smoke Marker Emissions During Flaming and Smoldering Phases of Laboratory Open Burning of Wildland Fuels, Aerosol Sci. Technol., 44(9), i–v, doi:10.1080/02786826.2010.499884, 2010.

Lin, G., Penner, J. E., Flanner, M. G., Sillman, S., Xu, L. and Zhou, C.: Radiative forcing of organic aerosol in the atmosphere and on snow: Effects of SOA and brown carbon, J. Geophys. Res. Atmospheres, 119(12), 2013JD021186, doi:10.1002/2013JD021186, 2014.

Lin, P., Aiona, P. K., Li, Y., Shiraiwa, M., Laskin, J., Nizkorodov, S. A. and Laskin, A.: Molecular Characterization of Brown Carbon in Biomass Burning Aerosol Particles, Environ. Sci. Technol., 50(21), 11815–11824, doi:10.1021/acs.est.6b03024, 2016.

May, A. A., Saleh, R., Hennigan, C. J., Donahue, N. M. and Robinson, A. L.: Volatility of Organic Molecular Markers Used for Source Apportionment Analysis: Measurements and Implications for Atmospheric Lifetime, Environ. Sci. Technol., 46(22), 12435–12444, doi:10.1021/es302276t, 2012.

Mazzoleni, L. R., Zielinska, B. and Moosmüller, H.: Emissions of Levoglucosan, Methoxy Phenols, and Organic Acids from Prescribed Burns, Laboratory Combustion of Wildland Fuels, and Residential Wood Combustion, Environ. Sci. Technol., 41(7), 2115–2122, doi:10.1021/es061702c, 2007.

Mohr, C., Lopez-Hilfiker, F. D., Zotter, P., Prévôt, A. S. H., Xu, L., Ng, N. L., Herndon, S. C., Williams, L. R., Franklin, J. P., Zahniser, M. S., Worsnop, D. R., Knighton, W. B., Aiken, A. C., Gorkowski, K. J., Dubey, M. K., Allan, J. D. and Thornton, J. A.: Contribution of Nitrated Phenols to Wood Burning Brown Carbon Light Absorption in Detling, United Kingdom during Winter Time, Environ. Sci. Technol., 47(12), 6316–6324, doi:10.1021/es400683v, 2013.

Mok, J., Krotkov, N. A., Arola, A., Torres, O., Jethva, H., Andrade, M., Labow, G., Eck, T. F., Li, Z., Dickerson, R. R., Stenchikov, G. L., Osipov, S. and Ren, X.: Impacts of brown carbon from biomass burning on surface UV and ozone photochemistry in the Amazon Basin, Sci. Rep., 6, 36940, doi:10.1038/srep36940, 2016.

Ofner, J., Krüger, H.-U., Grothe, H., Schmitt-Kopplin, P., Whitmore, K. and Zetzsch, C.: Physico-chemical characterization of SOA derived from catechol and guaiacol – a model substance for the aromatic fraction of atmospheric HULIS, Atmos. Chem. Phys., 11(1), 1–15, doi:10.5194/acp-11-1-2011, 2011.

Park, R. J., Kim, M. J., Jeong, J. I., Youn, D. and Kim, S.: A contribution of brown carbon aerosol to the aerosol light absorption and its radiative forcing in East Asia, Atmos. Environ., 44(11), 1414–1421, doi:10.1016/j.atmosenv.2010.01.042, 2010.

Saleh, R., Hennigan, C. J., McMeeking, G. R., Chuang, W. K., Robinson, E. S., Coe, H., Donahue, N. M. and Robinson, A. L.: Absorptivity of brown carbon in fresh and photo-chemically aged biomass-burning emissions, Atmos. Chem. Phys., 13(15), 7683–7693, doi:10.5194/acp-13-7683-2013, 2013.

Saleh, R., Robinson, E. S., Tkacik, D. S., Ahern, A. T., Liu, S., Aiken, A. C., Sullivan, R. C., Presto, A. A., Dubey, M. K., Yokelson, R. J., Donahue, N. M. and Robinson, A. L.: Brownness of organics in aerosols from biomass burning linked to their black carbon content, Nat. Geosci., 7(9), 647–650, doi:10.1038/ngeo2220, 2014.

Saleh, R., Marks, M., Heo, J., Adams, P. J., Donahue, N. M. and Robinson, A. L.: Contribution of brown carbon and lensing to the direct radiative effect of carbonaceous aerosols from biomass and biofuel burning emissions, J. Geophys. Res. Atmospheres, 120(19), 2015JD023697, doi:10.1002/2015JD023697, 2015.

Sang, X. F., Gensch, I., Kammer, B., Khan, A., Kleist, E., Laumer, W., Schlag, P., Schmitt, S. H., Wildt, J., Zhao, R., Mungall, E. L., Abbatt, J. P. D. and Kiendler-Scharr, A.: Chemical stability of levoglucosan: An isotopic perspective, Geophys. Res. Lett., 43(10), 2016GL069179, doi:10.1002/2016GL069179, 2016.

Scaramboni, C., Urban, R. C., Lima-Souza, M., Nogueira, R. F. P., Cardoso, A. A., Allen, A. G. and Campos, M. L. A. M.: Total sugars in atmospheric aerosols: An alternative tracer for biomass burning, Atmos. Environ., 100, 185–192, doi:10.1016/j.atmosenv.2014.11.003, 2015.

Schnitzler, E. G. and Abbatt, J. P. D.: Heterogeneous OH oxidation of secondary brown carbon aerosol, Atmos. Chem. Phys. 18(19), 14539–14553, doi:10.5194/acp-18-14539, 2018.

Deleted: Lu, Z., Streets, D. G., Winijkul, E., Yan, F., Chen, Y. Bond, T. C., Feng, Y., Dubey, M. K., Liu, S., Pinto, J. P. and Carmichael, G. R.: Light Absorption Properties and Radiative Effects of Primary Organic Aerosol Emissions, Environ. Sci. Technol., 49(8), 4868–4877, doi:10.1021/acs.est.5b00211, 2015.

Deleted: Discuss.

Deleted: 20

Deleted: 29

Deleted: 20

Deleted: 198

Schroeder, W., Prins, E., Giglio, L., Csiszar, I., Schmidt, C., Morisette, J. and Morton, D.: Validation of GOES and MODIS active fire detection products using ASTER and ETM+ data, Remote Sens. Environ., 112(5), 2711–2726, doi:10.1016/j.rse.2008.01.005, 2008.

Seinfeld, J. H. and Pandis, S. N.: Atmospheric chemistry and physics: from air pollution to climate change, John Wiley & Sons, Inc., New York., 1998.

Simoneit, B. R. T., Schauer, J. J., Nolte, C. G., Oros, D. R., Elias, V. O., Fraser, M. P., Rogge, W. F. and Cass, G. R.: Levoglucosan, a tracer for cellulose in biomass burning and atmospheric particles, Atmos. Environ., 33(2), 173–182, doi:10.1016/S1352-2310(98)00145-9, 1999.

Slade, J. H. and Knopf, D. A.: Multiphase OH oxidation kinetics of organic aerosol: The role of particle phase state and relative humidity, Geophys. Res. Lett., 41(14), 5297–5306, doi:10.1002/2014GL060582, 2014.

Smith, J. D., Kinney, H. and Anastasio, C.: Phenolic carbonyls undergo rapid aqueous photodegradation to form low-volatility, light-absorbing products, Atmos. Environ., 126, 36–44, doi:10.1016/j.atmosenv.2015.11.035, 2016.

Stein, A. F., Draxler, R. R., Rolph, G. D., Stunder, B. J. B., Cohen, M. D. and Ngan, F.: NOAA's HYSPLIT Atmospheric Transport and Dispersion Modeling System, Bull. Am. Meteorol. Soc., 96(12), 2059–2077, doi:10.1175/BAMS-D-14-00110.1, 2015.

Strigel, Andre M., Yau, Wallace W., Kirkland, Joseph J. and Bly, Donald D.: Modern Size-Exclusion Liquid Chromatography, Second Edition., John Wiley & Sons, Inc., 2009.

Sumlin, B. J., Pandey, A., Walker, M. J., Pattison, R. S., Williams, B. J. and Chakrabarty, R. K.: Atmospheric Photooxidation Diminishes Light Absorption by Primary Brown Carbon Aerosol from Biomass Burning, Environ. Sci. Technol. Lett., 4(12), 540–545, doi:10.1021/acs.estlett.7b00393, 2017.

Theodosi, C., Panagiotopoulos, C., Nouara, A., Zarmpas, P., Nicolaou, P., Violaki, K., Kanakidou, M., Sempéré, R. and Mihalopoulos, N.: Sugars in atmospheric aerosols over the Eastern Mediterranean, Progress in Oceanography, 163, 70–81, doi:10.1016/j.pocean.2017.09.001, 2018.

Urban, R. C., Lima-Souza, M., Caetano-Silva, L., Queiroz, M. E. C., Nogueira, R. F. P., Allen, A. G., Cardoso, A. A., Held, G. and Campos, M. L. A. M.: Use of levoglucosan, potassium, and water-soluble organic carbon to characterize the origins of biomass-burning aerosols, Atmos. Environ., 61, 562–569, doi:10.1016/j.atmosenv.2012.07.082, 2012.

Wang, X., Heald, C. L., Ridley, D. A., Schwarz, J. P., Spackman, J. R., Perring, A. E., Coe, H., Liu, D. and Clarke, A. D.: Exploiting simultaneous observational constraints on mass and absorption to estimate the global direct radiative forcing of black carbon and brown carbon, Atmos. Chem. Phys., 14(20), 10989–11010, doi:10.5194/acp-14-10989-2014, 2014.

Wang, X., Heald, C. L., Sedlacek, A. J., de Sá, S. S., Martin, S. T., Alexander, M. L., Watson, T. B., Aiken, A. C., Springston, S. R. and Artaxo, P.: Deriving brown carbon from multiwavelength absorption measurements: method and application to AERONET and Aethalometer observations, Atmos. Chem. Phys., 16(19), 12733–12752, doi:10.5194/acp-16-12733-2016, 2016.

Wang, X., Heald, C. L., Liu, J., Weber, R. J., Campuzano-Jost, P., Jimenez, J. L., Schwarz, J. P. and Perring, A. E.: Exploring the observational constraints on the simulation of brown carbon, Atmos. Chem. Phys., 18(2), 635–653, doi:10.5194/acp-18-635-2018, 2018.

Wang, Y., Hu, M., Lin, P., Guo, Q., Wu, Z., Li, M., Zeng, L., Song, Y., Zeng, L., Wu, Y., Guo, S., Huang, X. and He, L.: Molecular Characterization of Nitrogen-Containing Organic Compounds in Humic-like Substances Emitted from Straw Residue Burning, Environ. Sci. Technol., 51(11), 5951–5961, doi:10.1021/acs.est.7b00248, 2017.

Wong, J. P. S., Nenes, A. and Weber, R. J.: Changes in Light Absorptivity of Molecular Weight Separated Brown Carbon Due to Photolytic Aging, Environ. Sci. Technol., 51(15), 8414–8421, doi:10.1021/acs.est.7b01739, 2017.

Wooster, M. J.: Small-scale experimental testing of fire radiative energy for quantifying mass combusted in natural vegetation fires, Geophys. Res. Lett., 29(21), 2027, doi:10.1029/2002GL015487, 2002.

Zhang, X., Lin, Y.-H., Surratt, J. D., Zotter, P., Prévôt, A. S. H. and Weber, R. J.: Light-absorbing soluble organic aerosol in Los Angeles and Atlanta: A contrast in secondary organic aerosol, Geophys. Res. Lett., 38(21), L21810, doi:10.1029/2011GL049385, 2011.

Zhang, X., Lin, Y.-H., Surratt, J. D. and Weber, R. J.: Sources, Composition and Absorption Ångström Exponent of Light-absorbing Organic Components in Aerosol Extracts from the Los Angeles Basin, Environ. Sci. Technol., 47(8), 3685–3693, doi:10.1021/es305047b, 2013.

Zhang, Y., Forrister, H., Liu, J., Dibb, J., Anderson, B., Schwarz, J. P., Perring, A. E., Jimenez, J. L., Campuzano-Jost, P., Wang, Y., Nenes, A. and Weber, R. J.: Top-of-atmosphere radiative forcing affected by brown carbon in the upper troposphere, Nat. Geosci., 10(7), 486–489, doi:10.1038/ngeo2960, 2017.

Zhao, R., Mungall, E. L., Lee, A. K., Aljawhary, D. and Abbatt, J. P.: Aqueous-phase photooxidation of levoglucosan–a mechanistic study using aerosol time-of-flight chemical ionization mass spectrometry (Aerosol ToF-CIMS), Atmospheric Chem. Phys., 14(18), 9695–9706, 2014.

Zhao, R., Lee, A. K. Y., Huang, L., Li, X., Yang, F. and Abbatt, J. P. D.: Photochemical processing of aqueous atmospheric brown carbon, Atmos. Chem. Phys., 15(11), 6087–6100, doi:10.5194/acp-15-6087-2015, 2015.

Zhong, M. and Jang, M.: Dynamic light absorption of biomass-burning organic carbon photochemically aged under natural sunlight, Atmos. Chem. Phys., 14(3), 1517–1525, doi:10.5194/acp-14-1517-2014, 2014.

Zhou, S., Collier, S., Jaffe, D. A., Briggs, N. L., Hee, J., Sedlacek III, A. J., Kleinman, L., Onasch, T. B. and Zhang, Q.: Regional influence of wildfires on aerosol chemistry in the western US and insights into atmospheric aging of biomass burning organic aerosol, Atmos. Chem. Phys., 17(3), 2477–2493, doi:10.5194/acp-17-2477-2017, 2017.

Zhou, X. and Mopper, K.: Determination of photochemically produced hydroxyl radicals in seawater and freshwater, Mar. Chem., 30, 71–88, doi:10.1016/0304-4203(90)90062-H, 1990.

Table 1. Rate constants for the photo-enhancement and photo-bleaching of low- and high-MW WS BrC of wood smoke, with respect to photolysis (UVB and UVA) and OH oxidation. Note that for UVB photolysis and OH oxidation, the reported uncertainties represent the variability (±1σ) of multiple experiments (n=3) and that the rate constants for low-MW_1 and low-MW_2 BrC photobleaching corresponds to chromophores that were rapidly and slowly photobleached, respectively. Rate constants for UVA photolysis were previously reported in Wong et al. (2017).

	Fraction[a]	k_{OH}^{II}(M s^{-1})	k_{UVB}(s^{-1})	k_{UVA}(s^{-1})
BrC Photo-enhancement	Low-MW	-	-	$(5.3 \pm 1.5) \times 10^{-5}$
	High-MW	-	$(1.2 \pm 0.2) \times 10^{-4}$	$(9.2 \pm 1.4) \times 10^{-5}$
BrC Photo-Bleaching	Low-MW$_1$	-	$(3.5 \pm 0.7) \times 10^{-4}$	$(1.8 \pm 0.4) \times 10^{-5}$
	Low-MW$_2$	$(2.9 \pm 0.5) \times 10^{9}$	$(1.6 \pm 0.3) \times 10^{-5}$	
	High-MW		$(1.7 \pm 0.4) \times 10^{-5}$	$(1.5 \pm 0.6) \times 10^{-5}$

[a] High-MW BrC is defined as the sum of light absorptivity (Abs_{365}) for molecules with approximate molecular weights between 66K Da and 401 Da (i.e., SEC elution volumes between 8 and 15 mL) and low molecular weight fraction (low-MW) is defined as the sum of light absorptivity for molecules with approximate molecular weights of 400 Da and less (i.e., SEC elution volumes higher than 15 mL).

Deleted: are defined as

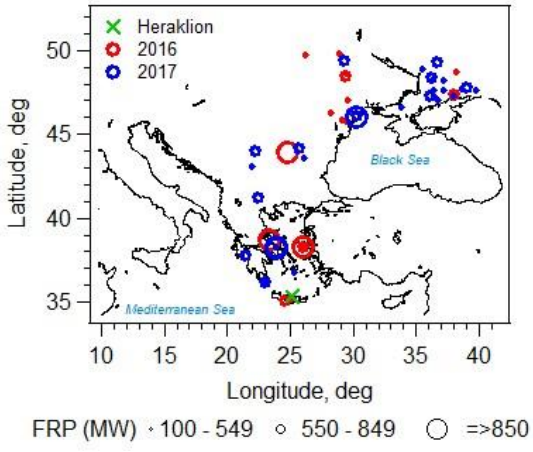

Figure 1. Locations of biomass burning events relevant to the current study, as detected by the Moderate Resolution Imaging Spectroradiometer (MODIS)/the Fire Information for Resource Management System (FIRES) (http://firms.modaps.eosdis.nasa.gov/firemap) during the fire seasons in 2016 (red circles) and 2017 (blue circles). The corresponding MODIS-measured fire radiative power (in megawatts, FRP) is represented by the size of the circle markers, and is provided as a rough proxy of biomass burning emission rate (Wooster, 2002). Wildfires with FRP less than 100 MW are not shown here. The location of the sampling site (Heraklion, Crete, Greece) is indicated by the green cross.

Deleted: of

Deleted: s

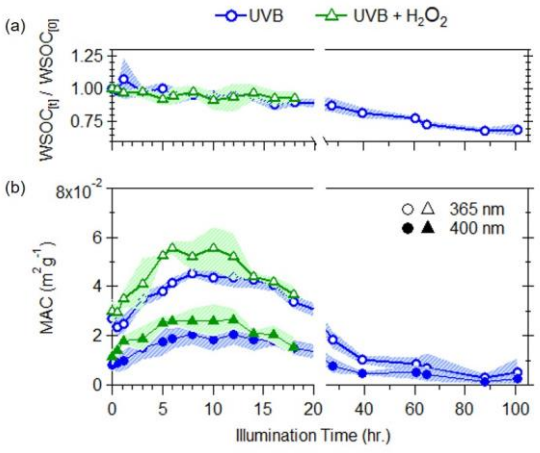

Figure 2. Effects of UVB photolysis (blue circles) and aqueous OH oxidation (green triangles) on: A) changes in WSOC, B) WSOC mass normalized absorption coefficient (MAC) at 365 nm (open markers) and 400 nm (filled markers). The shaded areas represent the variability (±1σ) of multiple experiments (n=3).

Deleted:

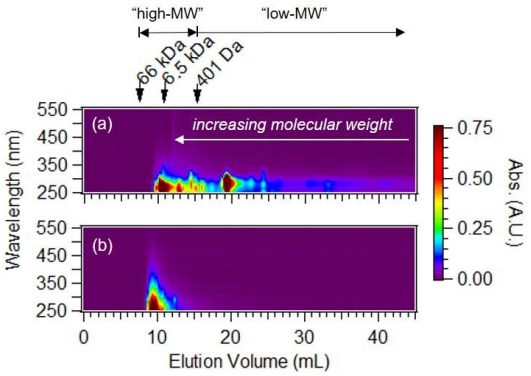

Figure 3. Molecular weight separated absorption spectra of a) unreacted water soluble BrC from laboratory generated wood smoke and b) ambient WS BrC from fresh biomass burning emissions (~ 1 hour of atmospheric transport) collected during the 2016 fire season in Crete, Greece. The elution volumes for high-MW and low-BrC and some calibration standards with known molecular weights are provided for reference. Note that molecular weight increases with decreasing elution volumes.

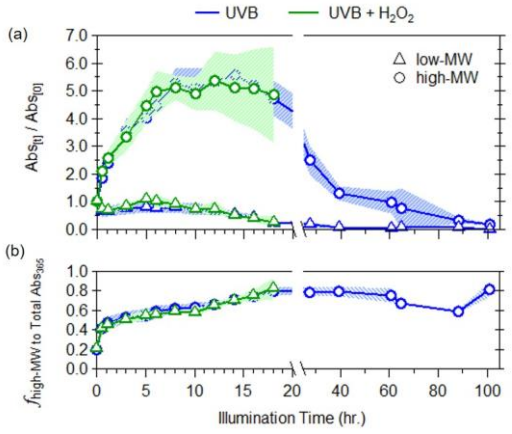

Figure 4. Changes in a) light absorption at a wavelength of 365 nm for low-MW (triangles) and high-MW (circles) BrC fractions and b) contribution of high-MW fraction to total light absorbance at 365 nm in WS smoke BrC due to UVB photolysis (blue) and aqueous OH oxidation (green). The shaded areas represent the variability (±1σ) of multiple experiments (n=3).

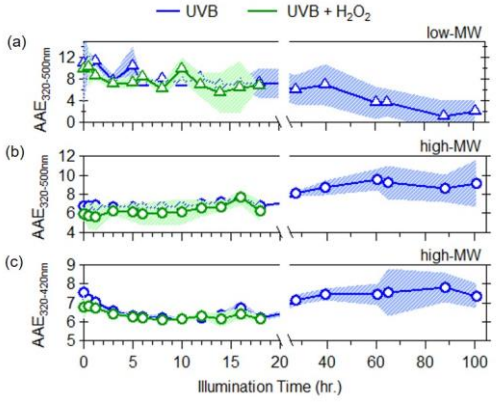

Figure 5 Evolution of AAE due to UVB photolysis (blue) and aqueous OH oxidation (green) for a) low molecular weight BrC (triangles), b) high molecular weight BrC (circles) from 320-500 nm, and c) from 320-420nm for high molecular weight BrC. The shaded areas represent the variability (±1σ) of multiple experiments (n=3).

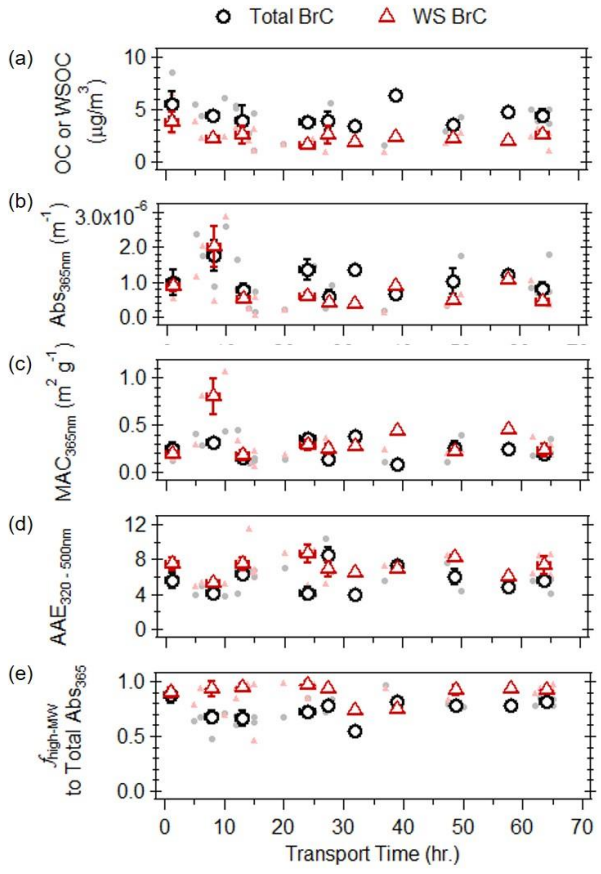

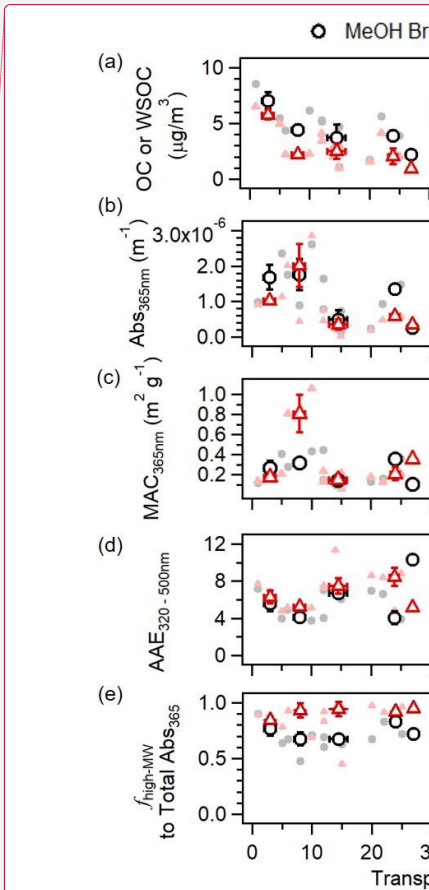

Deleted:

Figure 6. a) Organic carbon (OC) or water-soluble organic carbon (WSOC) concentrations, b) light absorption at 365nm, c) mass absorption coefficients at 365nm, d) AAE (in the wavelength range of 320 - 500 nm) and e) fractional contribution of high-molecular weight fractions to total light absorption as a function of atmospheric transport time, for MeOH (black circles) and water (red triangles) extractable portion of the ambient filters collected on Crete Island, Greece during the 2016 and 2017 fire seasons. The filled points are individual filter measurements, the open points represent the binned median values and the associated error bars represent the interquartile range.

Deleted: and

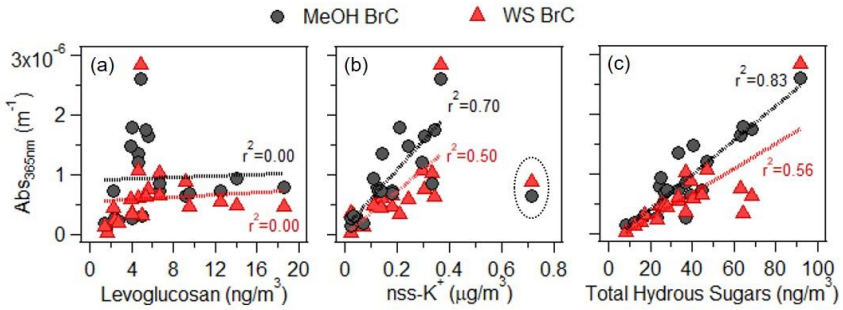

Figure 7. Correlations of light absorption at 365 nm for the MeOH (black circles) and water-soluble (red triangles) extractable portion of ambient filter samples that were impacted by biomass burning to ~~,~~ biomass burning tracers: a) levoglucosan, b) nss-K^+, and c) total hydrous sugars. For nss-K^+, outliers (circled points) were excluded ~~,~~ from the linear regression analysis.

Deleted: BB

Deleted: in

Supplement of

Atmospheric Evolution of Molecular Weight Separated Brown Carbon from Biomass Burning

J.P.S. Wong et al.

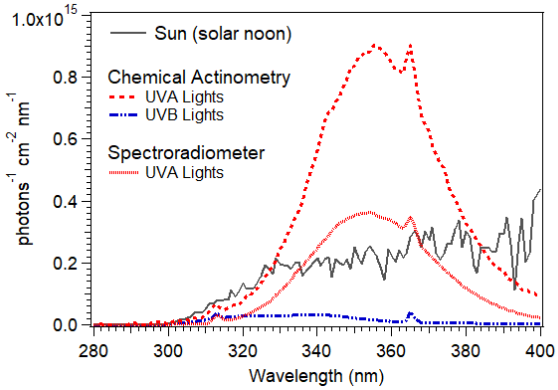

Figure S1. Measured photon flux in the photoreactor using chemical actinometry (dash lines) and spectroradiometer (solid line) for UVB (blue) and UVA lights (red; Wong et al., 2017). The actinic flux for a clear-sky summer day (black line) is included for comparison. The actinic flux was obtained from the National Center for Atmospheric Research (NCAR) "Quick TUV Calculator," available at http://cprm.acom.ucar.edu/Models/TUV/Interactive_TUV/ using the following parameters: Solar Zenith Angle = 0 deg, overhead ozone of 300 Dobson units, surface albedo of 0.1 and at 0 km attitude.

Section S1. OH Quantification Experiments

The following procedure for OH quantification using benzoate as a radical scanvenger was adapted from Zhou and Mopper (1990) and Anatasio and McGregor (2001). Sodium benzoate (0.1 – 1.0 µM; Sigma Aldrich) was added to WS wood smoke BrC extract solution with and without 1.5mM H_2O_2, in multiple 2 mL borosiliciate glass vials (sealed with Telfon-lined caps). The resulting vials were illuminated up to 18 hours in the photoreactor (equipped with 16 UVB lights), where at different times, a sample vial was removed and acidifed prior to injection with 2 drops of 1.0 M H_3PO_4 (Sigma Aldrich), to determine the concentration of *p*-HBA, using an High Performance Liquid Chromatrography (HPLC) system (GP40, Dionex), equipped with a C-18 column (Waters Symmetry®, 5 µm pore size, 4.6 mm diameter and 150 mm length), coupled to an UV/VIS spectrometer. The UV/VIS spectrometer consists of a liquid capillary waveguide (10 cm optical pathlength, World Precision Instrument), a deuterium tungsten halogen light source (DT-Mini-B, Ocean Optics), and an absorption spectrometer (USD4000, Ocean Optics). A two-solvent (A: acidified water at pH 2, using phosphate buffer; B: acetonitrile) multistep gradient elution was used to separate *p*-HBA from other isomers of hydroxybenzoic acid at a flow rate of 1.2 mL min^{-1}, as follows: isocratic at 80% A for 6.5 min, 80 to 50% A for 3.5 min; isocratic at 50% A for 1 min; 50% to 20% A in 4.5 min;

and then 20% to 80% A in 4.5 min. Absorption at λ = 256 nm were monitored for the detection of *p*-HBA (retention time, t_r =3.15 min). The response was calibrated by spiking *p*-HBA to WS BrC solution at various concentrations (i.e., standard addition method). The detection limit for *p*-HBA was determined to be ~ 200 nM, due to the absorbance at λ = 256 nm by BrC samples with the same elution time as *p*-HBA. We note that after only 30 min. of UVB irradiation, the observed production of *p*-HBA in WS BrC samples with 1.5 mM H_2O_2, is ten times of the detection limit. For each benzoate concentration, the formation rate of *p*-HBA ($R_{benzoate}$) was determined.

From the linear regression slope and y-intercept of the plot of 1/benzoate formation rate vs 1/benzoate concentration (Figure S3), two quanitites can be determined: the production rate of OH (P_{OH}, equation 1); and the apparent first-order rate constant of the reaction of BrC with OH (k'_{BrC}, equation 2):

$$P_{OH} = \text{y-intercept} \times Y_{pHBA} \quad (1)$$

$$k'_{BrC} = k_{benzoate} \times (\text{slope/y-intercept}) \quad (2)$$

where $k_{benzoate}$ is the reaction rate constant of benzoate with OH (5.9×10^9 M^{-1} s^{-1}; (Ross et al., 1994), and Y_{pHBA} is the yield of *p*-HBA from the reaction of benzoate with OH (0.17; Anastasio and McGregor, 2001). From these determined values, the steady-state concentration of OH ($[OH]_{ss}$) can be determined, as the OH production rate equals to the consumption rate by all OH scanvengers, which are WS BrC (R_{BrC}) and benzoate (R_{BrC}):

$$P_{OH} = R_{BrC} + R_{benzoate} \quad (3)$$

In which,

$$R_{BrC} = k'_{BrC}\,[OH]_{ss} \quad (4)$$

$$R_{benzoate} = k_{benzoate}[benzoate][OH]_{ss} \quad (5)$$

We note that the OH quantification experiments were conducted separately from the experiments where the effects of OH oxidation on WS BrC properties were examined to avoid measurement interference, as other products formed from the reaction of OH + benzoate readily absorb radiation in the same near UV region as WS BrC. As a result, the $[OH]_{ss}$ in the OH quantification experiment is lower to that of the WS BrC aging experiment, because of the presence of benzoate as an additional OH scanvenger, while the OH production rate reasons unchanged (Zhou and Mopper, 1990). As such, for the WS BrC aging experiments, the OH production rate equals to only to the consumption rate of WS BrC by OH (equation 3 where $R_{benzoate}$ = 0):

$$P_{OH} = k'_{BrC}\,[OH]_{ss} \quad (6)$$

Thus, using equation 6, for the WS BrC aging experiments, the $[OH]_{ss}$ in these experiments can be calculated from the the OH production rate and k'_{BrC} (equations 1 and 2, respectively). For these OH quantification experiments, the $[OH]_{ss}$ for solutions containing WS BrC with and without 1.5 mM H_2O_2 were determined to be 2.1×10^{-14} M and 1.55×10^{-14} M. The difference of these steady-state OH concentrations were taken to be due to the photolysis of the added 1.5 mM H_2O_2. From the reproductibility of the OH production rate for BrC with 1.5 mM H_2O_2, we estimate that the uncertainity of the $[OH]_{ss}$ is ~30%.

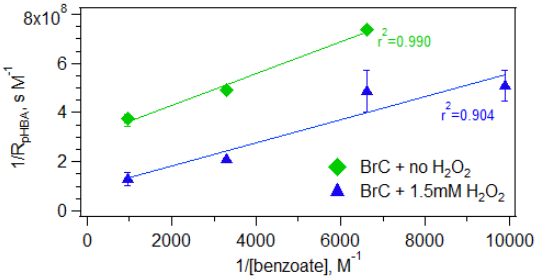

Figure S2. Relationship between the reciprocals of benzoate formation rate (R_{pHBA}) and the concentration of added benzoate in photolyzed WS wood smoke BrC solutions. Error bars represent variability (±1σ) of multiple experiments.

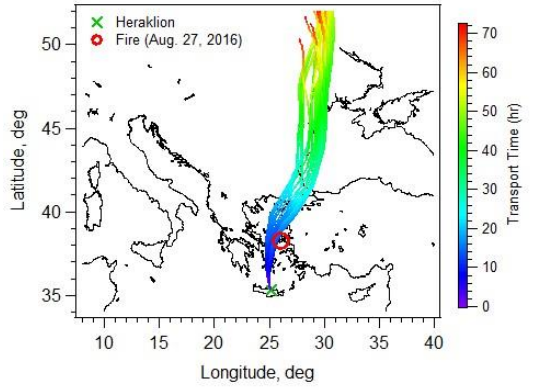

Figure S3. Multi-day biomass burning event on Chios from August 25 – 26th, 2016 (red circle) as detected by the Moderate Resolution Imaging Spectroradiometer (MODIS). Lines illustrate the 24 hourly airmass back trajectories from the sampling site (Heraklion, green cross) from July 27th, as computed using the HYSPLIT model for a total run time of 72 hours. The trace color for each line corresponds to the airmass transport time. For the field sample collected on July 27th, the estimated atmospheric transport time for the biomass burning BrC was approximately 18 hours.

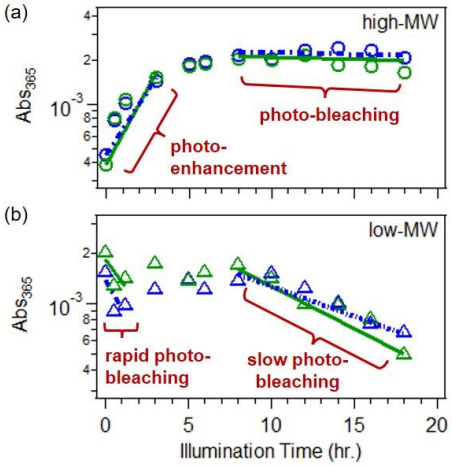

Figure S4. Light absorptivity (at 365 nm) of a) high-MW and b) low-MW WS BrC over the course of a representative experiment for aqueous OH oxidation (green) and UVB photolysis (blue). The lines illustrate the fitting of the photo-enhancement/photo-bleaching rate constants for the time periods highlighted. Note that the axis for light absorption is in log scale.

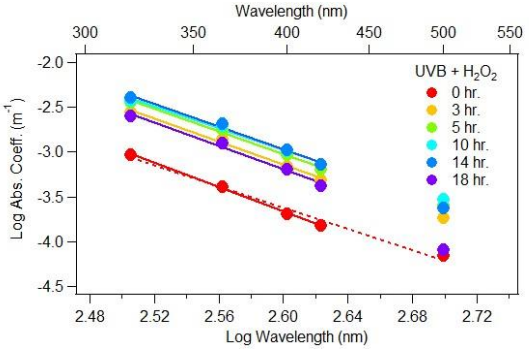

Figure S5. Log absorption coefficient vs. log wavelength over the course of a representative aqueous OH oxidation WS-BrC experiment. The linear fits determined between 320 - 420 nm (solid line) and 320 - 500nm (dash line) for BrC prior to photochemical aging (0 hr, dashed line) are illustrated.

Section 2. Atmsopheric Fate of Biomass Burning WS BrC

Aqueous OH Oxidation

The atmospheric lifetime ($\tau_{atm,\ OH\ oxd}$) due to aqueous OH oxidation (Table S1) is calculated using the experimentally determined second-order OH oxidation rate constant (k_{OH}^{II}, Table 1 in main text), and assuming a [OH]ss of 1×10^{-14} M, which represents the upper range of OH concentrations in fog/cloud droplets (Herrmann et al., 2010; Arakaki et al., 2013):

$$\tau_{atm,OH} = \frac{1}{k_{OH}^{II} \times [OH]_{ss}}$$

UV Photolysis

To estimate the atmsopheric lifetimes of processes leading to an increase (photoenhancement) and decrease (photobleaching) in the light absorptivity of different molecular weight fractions of BrC (τ_{atm}) with respective to photolysis (UVB and UVA), which are shown in Table S1, the experimentally observed lifetimes were calculated from the determined rate constants (Table 1 in main text). These observed lifetimes were converted to equivalent times in the atmosphere, assuming that the differences is only due to the ratio of photon fluxes in the photoreactor (F_{exp}) and the sun at Solar Noon (F_{atm}) in the UVB and UVA regions:

$$\tau_{atm,UV} = \tau_{exp,UV} \left(\frac{F_{\exp}}{F_{atm}}\right)$$

The photon fluxes determined for the UVB and UVA lights in the photoreactor were determined by integrating the corresponding flux (Figure S1) from 280 – 400 nm and 300 – 400 nm, respectively. For UVB lights, the photon flux ($F_{exp,\ UVB}$) was 2.57×10^{15} s^{-1} photon cm^{-2}, as determined using chemical actinometry. For UVA lights, the photon flux were determined using both chemical actinometry ($F_{exp,\ UVA,\ chemical\ actinometry} = 3.82 \times 10^{16}$ s^{-1} photon cm^{-2}) and spectroradiometer ($F_{exp,\ UVA,\ spectroradiometer} = 1.51 \times 10^{16}$ s^{-1} photon cm^{-2}) (Wong et al., 2017). For photon fluxes in the UVB and UVA regions from solar radiation, they were determined by integrating the flux in the same wavelength ranges mentioned above ($F_{atm,\ UVB} = 1.940 \times 10^{16}$ s^{-1} photon cm^{-2}; $F_{atm,\ UVA} = 1.939 \times 10^{16}$ s^{-1} photon cm^{-2}). This approach assumes that the quantum yields for BrC photoenhancement and photobleaching are wavelength independent. We also note that the calculated atmospheric lifetime with respect to photolysis assumes continuously exposure to solar photon flux corresponding to Solar Noon (i.e., no light/dark cycles).

Table S1. Estimated atmospheric lifetimes of processes leading to an increase (photoenhancement) and decrease (photobleaching) of the light absorpivity of small- and high-MW WS BrC, with respect to photolysis (UVB and UVA) and OH oxidation. Note that for UVB photolysis and OH oxiation, the rate contants for low-MW_1 and low-MW_2 photobleaching correspond to chromophores that were rapidly and slowly photobleached, respectively.

	Fraction	OH Oxidation[a]	Photolysis	
			UVB[a]	UVA[b]
BrC Photo-enhancement	Low-MW	-	-	3.2 – 8.1
	High-MW	-	1.5 ± 0.2	2.4 – 5.9
BrC Photo-Bleaching	Low-MW_1	-	0.7 ± 0.2	12 - 30
	Low-MW_2	9.8 ± 1.6	11 ± 1.6	
	High-MW	-	11 ± 2.3	14 - 36

[a] Uncertainties in atmospheric lifetime represents the variability (±1σ) of multiple experiments (n=3).
[b] Data obtained from Wong et al., (2017) where the range of atmospheric lifetimes calculated using photon fluxes determined using chemical actinometry and measured by spectroradiometer.

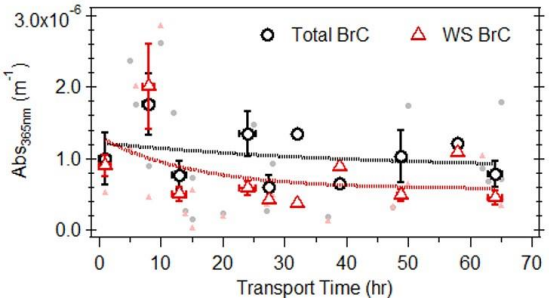

Figure S6. Fitted exponential decays to bulk light absorptivity at 365nm for MeOH (black circles) and WS (red triangles) extractable BrC in ambient biomass burning organic aerosols, sampled on Crete Island, Greece during the 2016 and 2017 fire seasons. The filled points are individual filter measurement and the open points represent the binned median values and the associated error bars represent the interquartile range.

Table S2. Linear regression slope (*m*), coefficient of determination (r^2), and p-value (*p*) between biomass burning tracers and bulk Abs_{365} for MeOH and WS BrC). The error represents the standard deviation (±1σ) associated with the slope.[a]

	Levoglucosan	nss-K^+	Total Hydrous Sugars
MeOH BrC			
m	(7.22 ± 0.34) × 10^{-9}	**(4.92 ± 0.76) × 10^{-6}**	**(2.88 ± 0.30) × 10^{-8}**
r^2	0.00	**0.70**	**0.83**

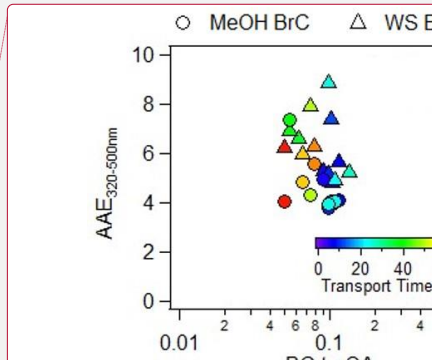

Deleted:
Figure S7. AAE (from 320 – 500nm) as a function of black carbon-to-organic aerosol (BC-to-OA) ratio for MeOH (circl and water (triangles) soluble portion of the ambient filters collected on Crete, Greece during the 2017 fire season. The co scale indicates the transport time associated with each filter sample, estimated from back trajectories calculated using HYSPLIT model. OA was estimated from the measured OC concentrations, using a conversion factor of 2 (Turpin and Li 2001).¶

p	0.835	**< 0.001**	**< 0.001**
WS-BrC			
m	$(9.84 \pm 0.30) \times 10^{-9}$	$\mathbf{(3.68 \pm 0.87) \times 10^{-6}}$	$\mathbf{(2.10 \pm 0.43) \times 10^{-8}}$
r^2	0.01	**0.50**	**0.56**
p	0.934	**< 0.001**	**< 0.001**

[a] Statistically significant correlations (p-value < 0.05) are bolded.

Reference

Anastasio, C. and McGregor, K. G.: Chemistry of fog waters in California's Central Valley: 1. In situ photoformation of hydroxyl radical and singlet molecular oxygen, Atmos. Environ., 35(6), 1079–1089, doi:10.1016/S1352-2310(00)00281-8, 2001.

Ervens, B.: Modeling the Processing of Aerosol and Trace Gases in Clouds and Fogs, Chem. Rev., 115(10), 4157–4198, doi:10.1021/cr5005887, 2015.

Herrmann, H., Hoffmann, D., Schaefer, T., Bräuer, P. and Tilgner, A.: Tropospheric Aqueous-Phase Free-Radical Chemistry: Radical Sources, Spectra, Reaction Kinetics and Prediction Tools, Chem. Phys. Chem, 11(18), 3796–3822, doi:10.1002/cphc.201000533, 2010.

Ross, A. B., Mallard, W. G., Helman, W.P., Buxton, G. V., Huie, R. and Neta, E. P.: NDRL-NIST Solution Kinetics Database - Version 2, NIST Standard Reference Data, Gaithersburg, M.D., 1994.

Turpin, B. J. and Lim, H.-J.: Species Contributions to PM2.5 Mass Concentrations: Revisiting Common Assumptions for Estimating Organic Mass, Aerosol Sci. Technol., 35(1), 602–610, doi:10.1080/02786820119445, 2001.

Wong, J. P. S., Nenes, A. and Weber, R. J.: Changes in Light Absorptivity of Molecular Weight Separated Brown Carbon Due to Photolytic Aging, Environ. Sci. Technol., 51(15), 8414–8421, doi:10.1021/acs.est.7b01739, 2017.

Zhou, X. and Mopper, K.: Determination of photochemically produced hydroxyl radicals in seawater and freshwater, Mar. Chem., 30, 71–88, doi:10.1016/0304-4203(90)90062-H, 1990.